Production of resonances and hadron jets in high-energy particle interactions and the structure of hadrons

V. G. Grishin

Joint Institute for Nuclear Research, Dubna

Fiz. Elem. Chastits At. Yadra **15**, 178–238 (January–February 1984)

A review is given of the main results of the investigation into production of resonances in hadron collisions and in deep inelastic lepton–nucleon interactions at high energies. It is shown that in all processes the dominant component among the secondary particles is resonances, which give direct information about the strong-interaction dynamics of quarks. The characteristics of hadron jets produced in hadron collisions, e^+e^- annihilation, and deep inelastic interactions are discussed. In the first approximation, they are the same and do not depend on the type of interaction. The theoretical interpretation of the intense resonance production and the universality of the hadron jets is considered in the framework of the additive quark model, which satisfactorily describes the transitions of hadrons into quarks and quarks into hadrons. From this there follows the existence of two characteristic quark dimensions ($r_N \sim 1/2m_\pi$ and $r_q \sim 1/m_N$) and rules of quark statistics for transitions of quarks into hadrons at large distances, where quantum chromodynamics is not valid.

INTRODUCTION

As a rule, many secondary hadrons are produced in collisions of high-energy particles ($E \gtrsim 10$ GeV). Their characteristics reflect both the nature of the interaction itself and the structure of the primary objects. The discovery of the quark structure of hadrons and the unification of the weak and electromagnetic interactions made it possible to regard all types of particle collision as due to the interaction of leptons and quarks.[1–2] In this connection, it is of interest to consider simultaneously multiparticle production processes in hadron, lepton–hadron, and lepton collisions.[3–16]

Multiparticle production in hadron collisions has already been studied for more than 30 years. In the beginning, there were the cosmic-ray experiments,[3] which were then followed in the sixties by investigations using accelerators in the Soviet Union, the United States, and Switzerland ($E \leqslant 2$ TeV).[4–12] In the intervening period, a huge amount of experimental information has been obtained about the characteristics of the secondary long-lived or stable particles ($\pi, K, \eta, N, \Lambda, \Sigma, \Xi, \Omega^-$), produced in hadron interactions.[1)] They are discussed in detail in the reviews of Refs. 4–12.

However, with the accumulation of these data it has gradually become clearer and clearer that the secondary long-lived hadrons are mainly the decay products of short-lived states (resonances) with lifetimes of 10^{-21}–10^{-23} sec. At first, there were indirect indications—the discovery of close correlations for pions of opposite sign ($\rho^0 \to \pi^+\pi^-$), the relatively large transverse momenta of secondary pions, etc.[5,7] In 1976 there were the first direct measurements of the intensity of the production of light meson resonances (ρ, ω, f) in inclusive processes, which showed that more than 50% of the secondary pions are the decay products of these resonances.[5–7]

This relatively late discovery of copious production of resonances at high energies ($E \gtrsim 10$ GeV) can be largely attributed to methodological reasons (see Sec. 1). Indeed, modern methods of detecting particles (nuclear emulsions, bubble chambers, electronic devices) have a spatial resolution of 1–100 μm, which makes it possible to study directly only the production characteristics of secondary particles with lifetimes $\tau \gtrsim 10^{-14}$ sec (with $c\tau \gtrsim 10^{-4}$ cm), i.e., pions, kaons, and baryons with $\tau \geqslant 10^{-14}$ sec. From their characteristics, using the known kinematics and dynamics of decays of resonances it is in principle possible to recover the characteristics of the production of the resonances (see Secs. 2 and 3).[17]

The copious production of resonances in multiparticle production processes shows that the characteristics of the secondary long-lived hadrons, studied for many years, are determined to a large degree, not by the dynamics of the processes, but by the known kinematics of the decays of the resonances.

In the present review, the main attention will therefore be devoted to the experimental results on the production of resonances as giving the most direct information about the dynamics and structure of hadrons (see Secs. 2 and 3). Therefore, we shall not consider the behavior of the production of long-lived hadrons (KNO scaling, Feynman scaling, correlation phenomena, etc.), which have been discussed in detail in numerous reviews.[5–8]

From the point of view of the interpretation of the obtained results, it is of interest to consider them in the framework of the semiphenomenological quark–parton model, combining both hard and soft hadron collisions (see Sec. 4). The theoretical basis of this model for hard collisions is quantum chromodynamics (QCD), which, however, does not give definite predictions for the fragmentation of quarks into hadrons, and the characteristics of this process are taken from experimental data.[1,2] For soft collisions, when the secondary hadrons have small transverse momenta ($p_\perp \lesssim 1$ GeV/c), QCD is not applicable, and in this case wide use is made of phenomenological models that take into account

[1)] We shall not discuss the production of charmed particles whose production probability is small compared with the ordinary and strange hadrons.

 0090-4759/84/010080-29$04.40

the quark–parton structure of the hadrons. In this respect, we give preference to the additive quark model, on the basis of which copious resonance production was predicted in 1973—and discovered experimentally only in 1976 (Refs. 5, 7, and 18–20).

The study of the characteristics of secondary hadrons in weak and electromagnetic interactions of high-energy particles has only just begun.[13–16] Only the first results have been obtained on the production of resonances in these processes; these show that, as in hadron collisions, their fraction is large (see Sec. 3). In addition, it is precisely in these processes that the quark nature of the strong interactions and the dynamics of quark transitions at large distances into hadrons, which cannot be described in the framework of QCD, are most clearly manifested. Therefore, we shall consider the available data on the characteristics of the hadron jets produced in deep inelastic lepton–nucleon collisions and in e^+e^- annihilation (see Sec. 3).

At the end, we summarize the main results of the investigations of the production of resonances and hadron jets at high energies.

1. METHODOLOGICAL PROBLEMS IN THE IDENTIFICATION OF RESONANCES AT HIGH ENERGIES

The most common way of studying the production of resonances at high energies is by analyzing the distributions of the secondary particles with respect to their effective masses (M) in inclusive processes of the type

$$a + b \to c + d + X, \tag{1}$$

where X denotes any possible set of secondary particles accompanying c and d. If particles c and d are the products of the decay of a resonance (R), then the reaction (1) takes place in two stages

$$a + b \to R + X \to c + d + X, \tag{2}$$

and in the distribution with respect to $M(c, d)$ one will observe a peak corresponding to the mass (M_R) and width [$\Gamma(R)$] of the resonance. This peak can be described by the well-known Breit–Wigner formula[17]:

$$\mathrm{BW}(M) = \frac{M^2}{q}\frac{M_R\Gamma}{(M^2-M_R^2)^2+M_R^2\Gamma^2}, \tag{3}$$

$$\Gamma = \Gamma_R\,(q/q_R)^{2l+1}\,(M_R/M), \tag{4}$$

where M_R and Γ_R are the mass and width of the resonance, l is the orbital angular momentum of the decay particles, q is their momentum in the rest frame of the resonance, and q_R is the momentum at $M = M_R$. Other expressions are sometimes used to describe resonances,[17] and they all give similar values of $\sigma(R)$ at the present accuracy of the experimental data.

To measure the production cross sections of the resonances [$\sigma(r_i)$] in the reactions (1) and (2), it is necessary to determine not only M_R and Γ_R but also the distribution of the background events with respect to M, especially in the region of the resonance peaks. Usually, the distribution with respect to $M(c, d)$ is approximated by the expression

$$\frac{dN}{dM} = \alpha\Phi_1(M) + \Phi_2(M)\sum_i \beta_i\,\mathrm{BW}(M) + \Phi_3(M)\sum_j \gamma_j F_j(M), \tag{5}$$

where $\Phi_i(M)$ are the background distributions and $F_j(M)$ are the distributions that take into account the contribution to dN/dM of resonances which decay into three or more particles among which the particles c and d are included. The coefficients α, β_i, and γ_j determine the production cross sections of the resonances and the background processes.

Identification of Ordinary "Broad" Resonances

In the low-energy experiments, when few particles ($n = 3$–4) were produced and all their characteristics were measured, the ratio $r = N(R)/N(\Phi)$ (signal/background) was, as a rule, significantly larger than unity. There was therefore no problem in finding the background curve in the region of the resonance. Uncertainties in its position ($\lesssim 10\%$) led to errors in the determination of $\sigma(R)$ at the level of a few percent.

On the transition to high energies ($E \gtrsim 10$ GeV), the situation becomes much more complicated. There are two reasons for this: the large number of particles ($\langle n\rangle \approx 10$–20) and the highly incomplete information about all the secondary particles (inclusive processes). The large number of secondary particles leads to the appearance of the so-called combinatorial background. The point is that even in the most favorable situation, when only resonances (for example, ρ^0 mesons) are produced in the reactions (1), their number is $N(\rho^0) = n/2$, and the number of "spurious" combinations in which pions from different ρ^0 mesons are combined is $N(\pi\pi) \sim n^2$ and $r \sim 1/n$. It can be seen from this that already when $n = 10$–20 the resonance peak may be only 5–10% of the background, and it will not be clearly revealed in the experimental distributions. In particular, it was for this reason that in the period 1968–1974, when there was a relatively low statistics ($\lesssim 5000$ events) in multiparticle production experiments, the "signal" from the $\rho^0 \to \pi^+\pi^-$ decays in the reactions (2) was not detected. And it was only after an increase in the statistics to tens of thousands of events that a "shoulder" was found in the region of the resonance [$r \approx 5$–10%], which, however, corresponded to a large cross section $\sigma(\rho^0)$.[19–24] As an illustration, Fig. 1 gives the distributions $dN/dM(\pi^+\pi^-)$ for π^-p interactions at p equal to 100, 200, and 360 GeV/c (event statistics of 770, 17 000, and 30 000, respectively).[24] The signals from the ρ^0 mesons are weakly expressed, though the cross section is $\sigma(\rho^0) = 8.5 \pm 0.4$ mb [$\sigma_{\mathrm{inel}}(\pi^-p) = 21$ mb] at $p = 200$ GeV/c. If it is borne in mind that in interactions with a large cross section there is also production of other resonances ($\rho^\pm, \omega, f, \Delta^{++}$, etc.), it becomes obvious that a large fraction of the secondary pions result from their decay. Therefore, the pions "carry" little information about the hadron-production dynamics.

We consider the problem of identifying resonances in the processes (2) when $r \sim 0.1$.[19–23] We begin with the experiments made at relatively low momenta ($p = 16$ GeV/c).[20,21] They were made by means of a hydrogen bubble chamber (2 m), in which all the secondary charged particles were detected (experiment with 4π geometry). The processes

$$\pi^+ + p \to \pi^+ + \pi^- + X \tag{6}$$

were studied.

In all, about 400 000 inelastic π^+p interactions were

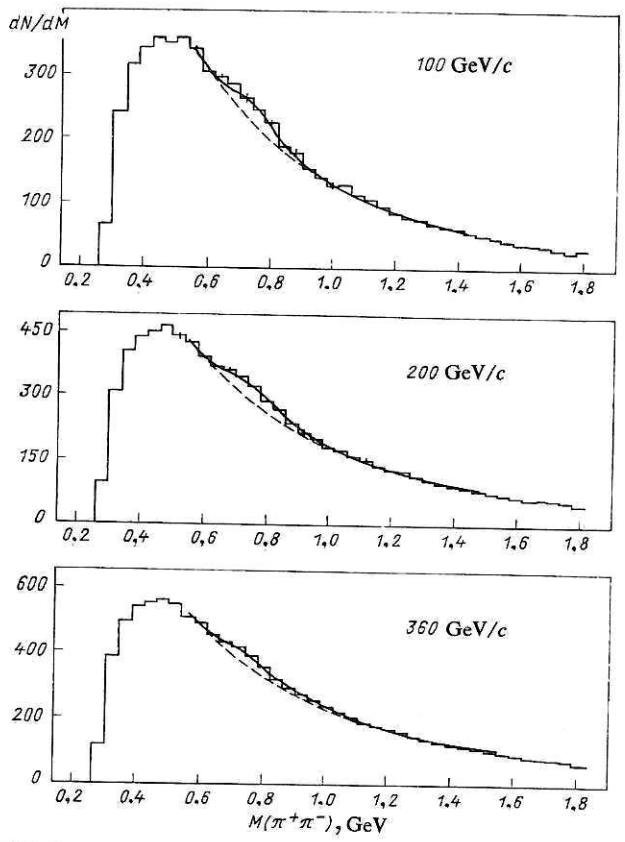

FIG. 1. Distributions of $\pi^+\pi^-$ pairs with respect to the effective mass in π^-p interactions at $p = 100$, 200, and 360 GeV/c. The broken curves represent the background processes, and the continuous curves are with allowance for ρ^0 mesons.

measured, and the errors in the measurement of the momenta of the secondary charged particles were 1–2%. Because of the relatively small number of secondary neutral pions at these energies [$\langle n(\pi^0)\rangle \lesssim 2$] and the high accuracy of the measurement of the momenta of the secondary particles, it was possible in about 50% of the events to determine the characteristics of all the secondary (charged and neutral) particles [exclusive channels of the reaction (6) without neutral particles and with the production of one π^0 meson or neutron]. The combination of all these advantages of the experiments at $p = 16$ GeV/c made possible a relatively good determination of the production cross sections for the various resonances (Table I).[21] However, even in this case the signal from the ρ^0 mesons appears only as a "shoulder" in the $M(\pi^+\pi^-)$ distribution (Fig. 2).[20] These data were approximated by the expression (5) without allowance for the "reflection" of other resonances [$F_j(M) = 0$]. Therefore, for ρ^0 mesons the interval of $M(\pi^+\pi^-)$ from 0.6 to 1.0 GeV was analyzed, and for f mesons $M = 0.9$–1.5 GeV. The background distribution was taken to be exponential,

$$\Phi_1(M) = \Phi_2(M)\exp(-AM - BM^2), \tag{7}$$

the values of M_R and Γ_R being free parameters. It was found that $M(\rho^0) = 0.768 \pm 0.001$ GeV, $\Gamma_R(\rho^0) = 0.154 \pm 0.002$ GeV and $M(f^0) = 1.284 \pm 0.010$ GeV, $\Gamma_R(f^0) = 0.225 \pm 0.038$ GeV. To within the errors, these are equal to the tabulated values of Ref. 17. As a result, the following values were determined: $\sigma(\rho^0) = 4.76 \pm 0.40$ mb and $\sigma(f^0) = 0.99 \pm 0.10$ mb [$\sigma_{\text{inel}}(\pi^+p) = 19.75 \pm 0.15$ mb and $\langle n_\pm \rangle \approx 4$]. The errors in the determination of $\sigma(R)$ are $\lesssim 10\%$ and are largely due to the uncertainty in the position of the background curve (7) at low signal levels.

In experiments made with a 2-m propane bubble chamber irradiated with π^- mesons with $p = 40$ GeV/c by means of the Serpukhov accelerator the processes

$$\pi^- + p \to \pi^+ + \pi^- + X \tag{8}$$

were studied, the statistics being 18 000 events (Fig. 3).[19] In this case, allowance was made for the "reflection" of the decays $\omega \to \pi^+\pi^-\pi^0[F_\omega(M)]$ in the spectrum $dN/dM(\pi^+\pi^-)$. The effect is found to be important for $M(\pi^+\pi^-) \leqslant m(\omega) - m(\pi^0)$ (Fig. 3).

The function $F_\omega(M)$ was found using the well-known expressions for the decay kinematics of the ω mesons with allowance for the matrix element[19]:

$$F_\omega(M) \sim M(\pi^+\pi^-)\int [\mathbf{p}_i \mathbf{p}_k]^2 dM^2(\pi^+\pi^0), \tag{9}$$

where $\mathbf{p}_{i,k}$ are the pion momenta. In addition, allowance was also made for the experimental resolution function:

$$\mathrm{BW}(M) = \frac{1}{\sqrt{2\pi}}\int \mathrm{BW}(m)\frac{1}{\sigma(m)}\exp\left[-\frac{(M-m)^2}{2\sigma^2(m)}\right]dm, \tag{10}$$

where $\sigma(m) = 0.071m - 0.019$ GeV.

TABLE I. Cross sections for the production of resonances in π^-p interactions at $p = 16$ GeV/c.*

Resonance	$\sigma(R_i)$, mb	Contribution to $\sigma(\pi^-)$, mb	$\frac{\sigma(R_i \to \pi^-)}{\sigma(\pi^+p \to \pi^-)}$, %
ρ^0	4.8±0.4	4.8±0.4	19.7±2.0
ρ^+	5.7±0.6	—	—
ρ^-	2.3±0.5	2.3±0.5	9.5±2.0
f	0.99±0.10	0.63±0.07	2.6±0.3
ω	4.0±0.7	3.7±0.6	15.2±2.5
η	1.5±0.3	0.44±0.09	1.8±0.3
η'	~0.1	~0.07	~0.3
Φ	~0.1	~0.01	~0.04
g_0	0.32±0.20	0.08±0.05	0.3±0.2
K^{*-} (890)	0.18±0.05	0.12±0.03	0.49±0.13
K^{*0} (890)	0.71±0.10	0.47±0.07	1.9±0.3
K^{*+} (890)	0.71±0.10	—	—
Δ^{++} (1232)	4.67±0.11	—	—

*$\sigma_{\text{inel}}(\pi^+p) = 20.0 \pm 0.2$ mb, $\sigma(R_i \to \pi^-) = 12.4 \pm 0.9$ mb $= 51 \pm 4\%$ of $\sigma_{\text{tot}}(\pi^+p \to \pi^-)$.

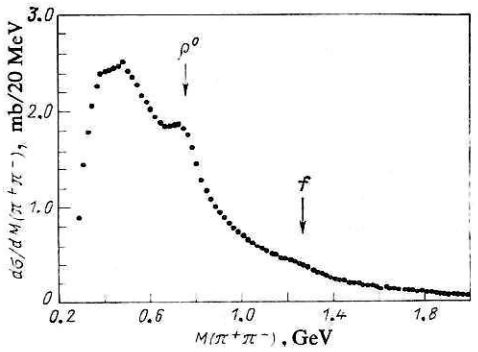

FIG. 2. Spectrum of effective masses of $\pi^+\pi^-$ pairs produced in π^+p interactions at $p = 16$ GeV/c.

The background distributions $\Phi_i(m)$ were assumed to be the same ($\Phi_i = \Phi_2 = \Phi_3$) and were taken in two variants in order to estimate the possible errors due to the choice of a definite type of $\Phi(M)$. The first variant used the distributions of identical pions,

$$\Phi_1(M) = \alpha(M)\frac{dN(\pi^+\pi^+)}{dM} + \beta(M)\frac{dN(\pi^-\pi^-)}{dM}, \qquad (11)$$

which were obtained in the same experiment $[\alpha(M)+\beta(M)+1]$. The advantages of $\Phi_1(M)$ are the allowance for the experimental resolution, the "reflections" of the three-particle decays of some resonances (for example, $A_0 \to \rho^{\mp}\pi^{\mp}$), and, partly, the dynamics of the background processes. It must be borne in mind that the interference of the identical particles increases the background when $M - m(2\pi) \lesssim 50$ MeV by 10–20%, and it is necessary to introduce a "suppression" of this effect on the basis of the $[\alpha(M), \beta(M)]$ available in the experimental data.[5] The distribution with respect to $M(\pi^+\pi^-)$ in the interval 0.3–2.3 GeV was approximated by the function (5) with allowance for (9), (10), and (11). As a result, it was found that $\sigma(\rho^0) = 7.9 \pm 0.7$ mb, $\sigma(\omega) = 7.2 \pm 0.8$ mb and $\sigma(f) = 1.3 \pm 0.5$ mb, with $\chi^2/N_{\text{deg.free.}} = 1.2$ [$\sigma_{\text{inel}}(\pi^-p) = 21.4 \pm 0.15$ mb and $\langle n_{\pm} \rangle = 5.52 \pm 0.04$].

In the second variant, the background was specified by an analytic expression, as at $p = 16$ GeV/c:

$$\Phi_2(M) = K\left(\frac{M_1}{M_0}\right)^a \exp(bM + cM^2), \qquad (12)$$

where $M_1 = m(\pi^+\pi^-) - 2m(\pi)$, $M_0 = 1$ GeV, K is a normalization coefficient, and a, b, c are free parameters. With this background distribution, the following values are obtained: $\sigma(\rho^0) = 7.4 \pm 0.8$ mb, $\sigma(\omega) = 6.0 \pm 0.8$ mb, and $\sigma(f) = 1.4 \pm 0.5$ mb with $\chi^2/N_{\text{deg.free.}} = 1.1$. To within the errors, the results do not disagree, and the difference between the mean values of $\sigma(R)$ does not exceed 8%, which can also serve as an estimate of the additional error associated with the choice of a definite form of the background distributions.

In both cases, it was found that $\sigma(\rho^0) \approx \sigma(\omega)$. The approximate equality of the cross sections for the production of ω and π mesons agrees with the predictions of the additive quark model[18] and disagrees with the multiperipheral models.[5]

The differential cross sections for resonance production with respect to the variables x, y, and $p_\perp^2$ can be determined by the same method of $\sigma(R_i)$.[2)] In this case, the total distribution of the $\pi^+\pi^-$ pairs with respect to $M(\pi^+\pi^-)$ is decomposed into several distributions with a value of the given variable for the $\pi^+\pi^-$ system in a definite interval (Δx, Δy, $\Delta p_\perp^2$). These distributions are then analyzed similarly in accordance with an expression of the type (5). Naturally, in this case there is an increase in the error in the determination of the cross sections, as well as in the uncertainty associated with the choice of the background distributions.[19–24]

The identification of the resonances and the determination of $\sigma(R)$ becomes a more and more difficult problem at higher energies. A characteristic example in this respect is provided by the experiments made at CERN using the accelerator with colliding proton beams at $E = 300$–2000 GeV.[22,23] The experiments were made by means of a magnetic spectrometer with proportional chambers. All charged secondaries were assumed to be pions, except for positively

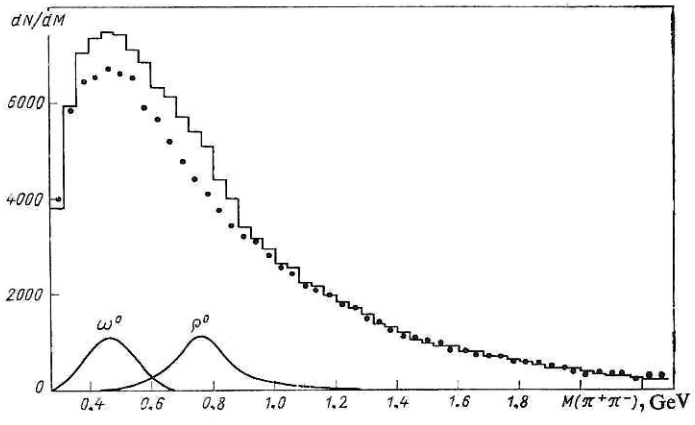

FIG. 3. Effective-mass spectrum of $\pi^+\pi^-$ pairs produced in π^-p interactions at $p = 40$ GeV/c. The histogram represents the experiment; the points, background processes; and the continuous curves, the signals from the ρ and ω mesons.

[2)]Here $x = 2p_\parallel^*/\sqrt{s}$, $p_\parallel^*$ is the longitudinal c.m.s. momentum of the resonance, $\sqrt{s}$ is the total energy, and $y = \frac{1}{2}\ln\frac{E^*(R)+P_\parallel^*(R)}{E^*(R)-p_\parallel^*(R)}$

charged particles with $|x| \gtrsim 0.4$, which are protons with a probability of more than 80%. To obtain a good resolution with respect to $M(\pi\pi)$ ($\Delta M/M \lesssim 5\%$), pions with $p \geqslant 0.3$ GeV/c and $\Delta p/p \leqslant 0.3$ were selected. As a result of these selection conditions, only about 40% of the charged secondaries were considered in the construction of the spectra dN/dM. Corrections for the efficiency of detection of events and particles were introduced on the basis of Monte Carlo calculations using data from other experiments. The systematic errors in $\sigma(R)$ associated with the determination of the efficiency were estimated to be at the 10% level.[23] The probability of detecting ρ^0 mesons varied from 0.13 ($\sqrt{s} = 23.6$ GeV) to 0.21 (63.0 GeV). At each energy ($\sqrt{s} = 23.6$, 30.6, 44.6, 52.8, and 63 GeV) about 25 000 events were analyzed.

The method described above was used to obtain the spectra of the $\pi^+\pi^-$ pairs with respect to their effective masses at different energies (for example, $\sqrt{s} = 52.8$ GeV, Fig. 4). For the background distribution, the distributions of pion pairs from different events normalized to the region 2–4 GeV, where significant dynamic correlations are not expected, were used. The difference between these distributions is shown in Fig. 5. The dN/dM distributions (Fig. 5) were analyzed by means of the expression (5) in the interval from 0.5 to 1.5 GeV with allowance for the Breit–Wigner function for the ρ mesons and the instrumental resolution and efficiency. The background distribution was taken in the polynomial form

$$\Phi^{(1)}(M) = a_1/M + a_2/M^2. \tag{13}$$

The other background distribution

$$\Phi^{(2)}(M) = a_3 \exp(-a_4 M) \tag{14}$$

decreases $\sigma(\rho^0)$ by 25%.[23] The effect associated with the reflection of the $\omega \to \pi^+\pi^-\pi^0$ decays was studied under the assumption $\sigma(\omega) = \sigma(\rho^0)$.[18] It was found that in this case $\sigma(\rho^0)$ increases by 20%.[23] These changes in the values of $\sigma(\rho^0)$ have opposite signs. Therefore, the authors gave the values of $\sigma(\rho^0)$ obtained usng $\Phi^{(1)}(M)$, indicating only the statistical errors. For example, at $\sqrt{s} = 63$ GeV, $\sigma(\rho^0) = 20.9 \pm 2.4$ mb and $\langle n(\rho^0)\rangle = 0.59 \pm 0.07$. At low energies ($\sqrt{s} = 24$ GeV), the value $\sigma(\rho^0) = 12.4 \pm 1.7$ mb obtained in this experiment agrees with the data of other experiments made by means of bubble chambers at the Fermilab accelerator (Batavia).

Consideration of typical experiments[19–24] on the determination of $\sigma(R_i)$ for meson resonances (ρ, ω, f) shows that at high energies the large number of "spurious" combinations (combinatorial background) means that $\sigma(R)$ cannot be measured with an error of less than 10%. However, in a number of cases one can appreciably reduce this background by, for example, studying the production of resonances through their rare decays in which there are no pions. In this case, the number of spurious combinations is small [$\langle n(R_i)\rangle \lesssim 1$]. A good example in this respect is provided by reactions of the type

$$a + b \to \rho^0(\omega^0) + X \to \mu^+\mu^-(e^+e^-) + X, \tag{15}$$

in which the background processes (direct lepton pairs, hadron decays into leptons, etc.) make up only 10% of the resonance peak in the distribution with respect to $M(\mu^+\mu^-)$.[25] This makes it possible to determine $\sigma(R_i)$ with an error of 5–10%. The probability of $\rho(\omega)$ decays into lepton pairs is 10^{-4} times smaller than through the channel $\rho^0 \to 2\pi$ or $\omega \to 3\pi$. Therefore, the reactions (15) can be studied only by means of the electronic method. Unfortunately, there are as yet no measurements of cross sections of processes of the type (15) in the complete range of variation of x.

Identification of Baryon and Strange Resonances

Somewhat different problems arise in the investigation of the production of baryon and strange resonances, the fraction of which at $E \lesssim 400$ GeV is still small ($\lesssim 10\%$) in the interactions of ordinary particles (pions and nucleons). In this case, it is very important to have a correct identification of the particle species. In bubble chambers, charged pions, kaons, and protons can be distinguished by means of ionization only for $p \lesssim 1.5$ GeV/c. At higher momenta, the particle species is, as a rule, unknown. For the construction of the effective-mass distributions of the pions, which constitute $\gtrsim 80\%$ of all secondaries, an "incorrrect identification" of the fast particles ($K^\pm, p \to \pi^\pm$) in a relatively small fraction has a weak influence on the resonance peaks but increases the background. The situation is greatly complicated when baryon resonances are investigated.

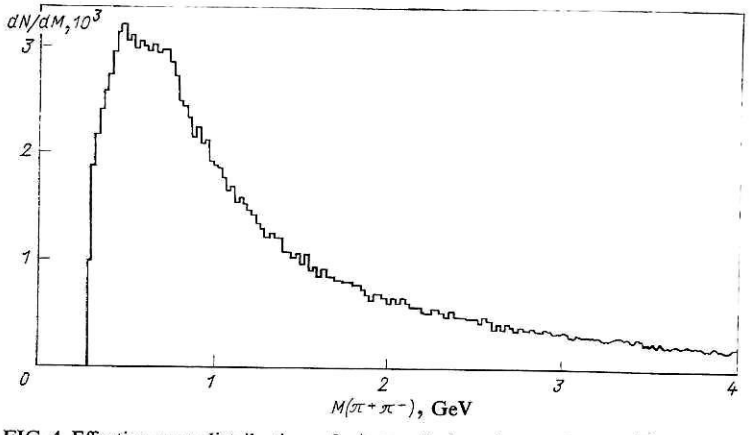

FIG. 4. Effective-mass distributions of $\pi^+\pi^-$ pairs in pp interactions at $\sqrt{s} = 52.8$ GeV.

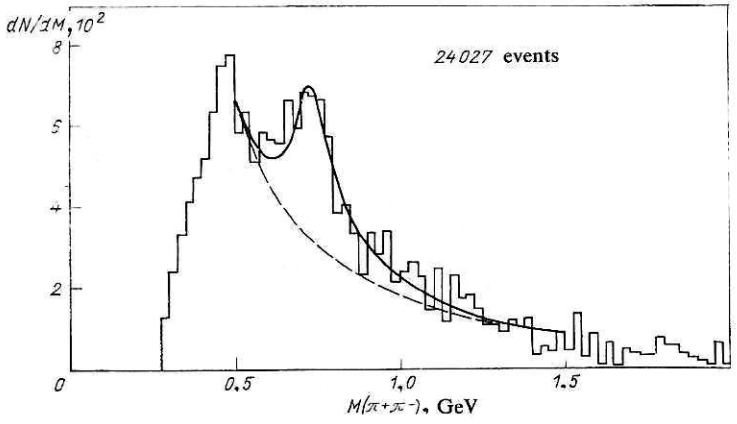

FIG. 5. Effective-mass distributions of $\pi^+\pi$ pairs after subtraction of background processes (pp, $\sqrt{s} = 52.8$ GeV). the broken curve is the background distribution (13), the continuous curve represents Eq. (5) with allowance for ρ^0 production, and the histogram represents the experiment.

As an example, we consider the experimental studies of the processes

$$K^-(\pi^\pm) + p \to \Delta^{++}(1232) + X \to p + \pi^+ + X \qquad (16)$$

at $p = 16$ and 32 GeV/c.[26] In this case, the protons were identified by means of ionization in a hydrogen bubble chamber when $p \lesssim 1.4$ GeV/c. Their fraction among the total number of secondary protons was about 40%. The $\pi^- p$ interaction cross sections $\sigma[\Delta^{++} \to p(\lesssim 1\ \text{GeV}/c)\pi^+]$ $= 0.63 \pm 0.05$ mb was found to be one third of the total cross section $[\sigma(\Delta^{++}) = 2.00 \pm 0.13$ mb]. It was determined by constructing the distributions with respect to the effective mass $M(p\pi^+)$ both for events with an identified proton and without one. In the latter case, it was assumed that each of the positively charged particles with $p \gtrsim 1$ GeV/c could be a proton or a π^+ mesons (Fig. 6). The background distribution was chosen in the form

$$\Phi(M) \sim q e^{-aM}, \qquad (17)$$

where q is the momentum of the decay particles in the rest frame of the resonance. The distributions clearly reveal a broad peak in the region of the Δ resonance with a much larger background "pedestal" than in the events with an identified proton. Analysis of these distributions using Eq. (5) gives the values of $\sigma(\Delta^{++}) = 4.67 \pm 0.11$ mb, 2.00 ± 0.13 mb, and 1.76 ± 0.07 mb for the $\pi^+ p$, $\pi^- p$, and $K^- p$ interactions at $p = 16$ GeV/c and 1.75 ± 0.15 mb for $K^- p$ collisions at $p = 32$ GeV/c.[26]

The values of $M(\Delta^{++})$ and $\Gamma(\Delta^{++})$ were found to be 1.228 ± 0.001 GeV and 0.123 ± 0.003 GeV for $\pi^+ p$ interactions and agreed to within the errors with the values tabulated in Ref. 17.

The errors in $\sigma(\Delta^{++})$ given at the 5% level are clearly too low, since they do not take into account the uncertainty in the describing of the background curve and its "distortion" due to incorrect identification of particles ($\pi^+ \to p$) in practically every event. Nevertheless, a resonance signal is revealed despite this huge admixture and the "incorrectly" identified particles. They probably give a "smooth" background in the region of the Δ^{++} resonance. Naturally, an approach of this type can also be used to determine the $\sigma(R)$ of strange resonances [for example, $K^{0*}(890) \to K^\pm \pi^\mp$], when complete identification of the $K^\pm$ mesons is impossible, and their fraction among the secondaries is 20–40% ($K^\pm p$ interactions).

With increasing energy, the efficiency of this method of identifying resonances will decrease because of the increased number of secondaries. In this case, as in the study of the production of ρ^0 (ω^0) mesons, it may be preferable to investigate rare decays of the baryon resonances:

$$\Delta^*(N^*) \to N + \rho^0(\omega^0) \to N + \mu^+\mu^-(e^+e^-), \qquad (18)$$

$$\Delta^*(N^*) \to N + \gamma \qquad (19)$$

etc.[17]

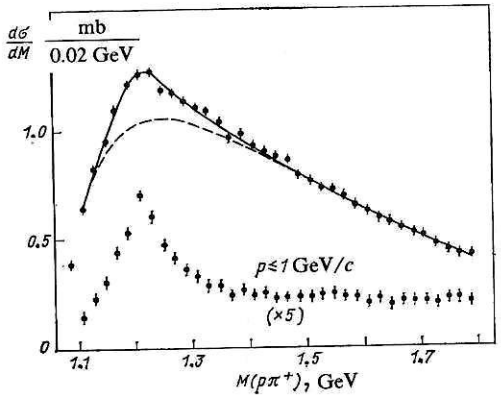

FIG. 6. Effective-mass spectrum of $\pi^+ p$ systems produced in Kp interactions at $p = 32$ GeV/c. The broken curve is the background distribution, and the continuous curve takes into account the production of the Δ^{++} resonance. Below, the distribution with respect to $M(\pi^+ p)$ in events with an identified proton ($p \lesssim 1.0$ GeV/c).

Identification of Neutral Strange Particles

In large bubble chambers, decays of secondary neutral strange particles can be detected: $\Lambda^0 \to p\pi^-$ and $K^0_S \to \pi^+\pi^-$. This makes it possible to obtain data on the production of resonances that decay with the participation of Λ^0 particles and K^0 mesons. The main background processes in the identification of Λ^0 and K^0 particles are e^+e^- conversion pairs produced by photons arising from the decay of secondary neutral pions ($\pi^0 \to \gamma\gamma$). At $E \lesssim 400$ GeV, the angle between

the electron and positron of the pair ($\theta_1 \sim m_e/E_\gamma$) is still, as a rule, appreciably smaller than the angle between the hadrons resulting from the decay of the Λ^0 and K^0 particles ($\theta_2 \sim 0.1$ GeV$/E_{\Lambda^0(K^0)}$). Therefore, at these energies one can with good efficiency (better than 80%) identify decays of neutral strange particles. With increasing energy, an ever larger fraction of the neutral particles will decay outside the effective volume of the chamber, and the identification of the detected decays will become an ever more complicated problem because of the small angle between the secondary particles ($\theta_2 \sim 0.1/E_{\Lambda(K)}$) and the large number of background e^+e^- pairs.

At the existing energies of the accelerators of ordinary type $\langle n(\Lambda^0)\rangle \lesssim 0.3$ and $\langle n(K^0)\rangle \lesssim 1.0$, and therefore the combinatorial background is also less than in the study of the production of ρ and ω mesons. In addition, the first strange resonances $K^*(890)$ and $\Sigma^*(1385)$, which decay into $K\pi$ and $\Lambda\pi$, have small widths [$\Gamma(K^*) = 50$ MeV and $\Gamma(\Sigma^*) = 35$ MeV], which also makes it possible to improve the signal/background ratio. Therefore, the accuracy in the determination of the $\sigma(R)$ of these resonances by means of the chamber method is usually basically determined by the statistics of the events with detected decays of strange particles, since $\sigma(\Lambda^0) \sim 1.5$ mb and $\sigma(K^0_S) \approx 2$–3 mb.

As an illustration, we give the results of a study of the production of $K^{*+}(892)$ and $\Sigma^+(1385)$ in π^+p and K^+p interactions at $p = 32$ GeV$/c$ by means of the hydrogen bubble chamber MIRABELLE.[27] Altogether, measurements were made of 101 499 inelastic K^*p interactions and about 5500 inelastic π^+p collisions. The substantial event statistics in the K^+p interactions made it possible to detect and measure in the effective volume of the chamber about 10 500 decays of K_S mesons and about 2700 decays of Λ hyperons. The procedure described above for analyzing the effective-mass distributions $M(K\pi)$ and $M(\Lambda\pi)$ yielded $\sigma[K^{*+}(890)] = 3.4 \pm 0.3$ mb and $\sigma[\Sigma^{*+}(1385)] = 0.12 \pm 0.02$ mb. In both cases, a resonance peak could be clearly seen in the distributions ($r \gtrsim 1$).

Because of the relatively low statistics of analyzed events in π^+p interactions the $K^{*+}(890)$ and $\Sigma^+(1385)$ production cross sections were determined with large errors: $\sigma(K^{*+}) = 1.1 \pm 0.6$ mb and $\sigma(\Sigma^{*+}) = 0.20 \pm 0.08$ mb.[27] Thus, the accuracy in the measurement of $\sigma(R_i)$ for resonances that decay with the participation of Λ^0 and K^0 particles at $E \lesssim 400$ GeV is largely determined by the event statistics, and the influence of the combinatorial background and the other background processes is much less than in the study of the production of meson resonances and Δ isobars.

The chamber method was used to investigate the production of the resonances $\Xi^*(1530)$ with strangeness $S = -2$. They were studied in the reaction

$$K^- + p \to \Xi^- + \pi^+ + X \to \Lambda^0 + \pi^- + \pi^+ + X \qquad (20)$$

at $p = 16$ GeV$/c$.[28] Altogether, an analysis was made of 410 000 inelastic K^-p interactions detected by means of a hydrogen chamber (CERN, Geneva) and the number of Ξ^- hyperons found was 861 [$\sigma(\Xi^-) = 135 \pm 15\,\mu$b]. The distribution with respect to the effective masses $M(\Xi^-\pi^+)$ revealed a clear peak ($r \geqslant 3$!) with $M(R) = 1535 \pm 4$ MeV and $\Gamma(R) = 14 \pm 5$ MeV. Application of the standard procedure yielded $\sigma[\Xi^{*0}(1530)] = 32 \pm 5\,\mu$b, which is a record for the study of the production of resonances with such a small cross section.

Thus, data have now been obtained on the production of resonances in hadron interactions in a wide range of energies ($E \lesssim 2000$ GeV). Their total cross sections have been measured in the range from a few microbarns to tens of millibarns. Most of the secondaries are produced by decays of resonances, which means that it is necessary to develop methods of identifying them in order to study the particle-interaction dynamics.

The various methodological problems associated with the measurement of $\sigma(R_i)$ can be reduced to three main ones, which are characteristic for all types of particle interaction.

The first problem is associated with the large number of secondary particles of a given species (n_i). For $E \lesssim 2000$ GeV, this applies largely to the identification of the meson resonances (p, ω, etc.). In this case, the large combinatorial background (about n_i^2) has the consequence that even in the case of large cross sections [$\sigma(R_i) \sim 10$ mb] the signal from the resonances is only 5–10% of the background and exact measurement of $\sigma(R_i)$ becomes difficult. With increasing energy, this problem also arises for other particles (K, N, $\bar{N}$, etc.). One of the possible ways out is to measure $\sigma(R_i)$ in rare decays of resonances [for example, $\rho^0(\omega^0) \to \mu^+\mu^-(e^+e^-)$] using the electronic method. This will be possible as long as $\langle n(R_i)\rangle \lesssim 1$–5. At even higher energies ($E \gtrsim 10^3$ TeV), this method of resonance identification also becomes ineffective.

The second methodological difficulty is associated with the absence of complete identification of the charged secondaries. In the first place this applies to measurement of the production cross sections of nucleon isobars and strange resonances which decay into charged particles ($K^{*0} \to K^\pm\pi^\mp$, $\Sigma^{*\mp} \to \Lambda^0\pi^\mp$, etc.). In this case, the combinatorial background is less than in the determination of the meson-resonance cross sections ($E \lesssim 400$ GeV), but the absence of information about the species of the secondary particles may lead to additional systematic errors difficult to estimate (see the discussion of the method of identification of the Δ isobar).[26] Of course, it is in principle possible by means of electronic methods of particle detection to obtain more complete information about the species of secondary particles than it is in experiments made using the chamber method. However, as yet this is in practice possible only for a relatively small range with respect to the variables x and $p_\perp^2$.

Specific features of the identification of resonances arise in the study of neutral strange particles. With increasing energy in this case, the background from conversion e^+e^- pairs makes the identification of the Λ^0 and K^0 particles more and more difficult. In this connection, it is necessary to develop electronic methods of detecting such particles with suppression of the background from the $\gamma \to e^+e^-$ processes.

A new region of energies is now available for experimental investigations since the commissioning of the accelerator with colliding proton and antiproton beams at CERN. Their energies 270×270 GeV in the c.m.s. correspond to $E \approx 150$ TeV in the laboratory system for accelerators of the ordinary type with a fixed target. The physicists

that investigate cosmic-ray interctions[3,4] have some experience of working at these energies. However, it is clear that detailed study of strong interactions is only possible using accelerators. The mean multiplicity of the charged secondaries is $\langle n_{\pm} \rangle = 27 \pm 2$ at $E \sim 150$ TeV. It is approximately 2.5 times greater than at $E = 2$ TeV for pp collisions. At such a multiplicity, the methodological difficulties of identifying light resonances that decay into two or three particles increase ($\sim n^2$). It is quite possible that at these energies only the characteristics of groups of particles will be studied without particularization of their origin, together with the study of the production of heavy resonances (or clusters) decaying into many particles ($n_{\pm} \gtrsim 5$). Of course, for events with low multiplicity ($n_{\pm} \lesssim \langle n_{\pm} \rangle$) the production of light resonances will be investigated, as at $E \lesssim 2$ TeV.

We note finally that the methodolological problems of idetifying resonances produced in weak and electromagnetic interactions of leptons with nucleons in e^+e^- collisions are just the same as the ones considered above.

2. PRODUCTION OF RESONANCES IN SOFT HADRON COLLISIONS

At the present time, the most complete information about the production of resonances has been obtained in the study of soft hadron collisions at $E < 2$ TeV.

Some results on the production of resonances at relatively low energies ($E < 100$ GeV) have already been reviewed.[5-7] In recent years, new results have been obtained on the production of vector and tensor mesons ion $K^{\pm} p$ interactions at $p = 32$ and 70 GeV/c.[27] In this connection, we shall merely recall the main results at such energies and dwell in more detail on the recent Kp experiments, which are of interest for testing theoretical models. We devote our main attention to the results at $E > 100$ GeV.

Total Cross Sections and Mean Multiplicities of Resonances

A compilation of data on the $\rho^0, f^0, K^*(890)$, and φ meson production cross sections in pp, $\bar{p}p$, and $\pi^{\pm} p$ interactions at $E < 2$ TeV is shown in Fig. 7.[7,29] We first consider the data obtained in pp interactions. In this case, the meson resonances are produced mainly in the central region ($|y^*| \lesssim 2$). For example, $p \to \rho^0$ fragmentation is approximately five times less than $\sigma_c(pp \to \rho^0)$ in the central region.[5,23] It may therefore be assumed that the energy dependence of $\sigma(R_i)$ is largely determined by the growth of the cross section in the central region. The value of $\sigma(\rho^0, s)$ was found to be

$$\sigma_{\rho} = (0{,}38 \pm 0{,}02) \ln^2 s - (2{,}1 \pm 0{,}4), \qquad (21)$$

where σ_{ρ} is measured in mb and s in GeV^2 (the continuous curve in Fig. 7).[23] A similar dependence of $\sigma(R_i, s)$ on s describes satisfactorily $\sigma(f^0, s)$ and $\sigma(K^*, s)$. The somewhat different behavior of $\sigma(\rho^0)$ for $\pi^{\pm} p$ interactions is due to the relatively low energies at which the data were obtained and the large fragmentation cross sections $\sigma_f(\pi^{\pm} \to \rho^0)$, which are 30–50% of $\sigma(\rho^0)$.[5] The results obtained show that at $E \leqslant 100$ GeV an important part is played by processes of annihilation [see, for example, $\sigma(\rho^0)$ for $\bar{p}p$ interactions in Fig. 7] and fragmentation of the primary particles, and therefore the transition to the "asymptotic" regime begins at

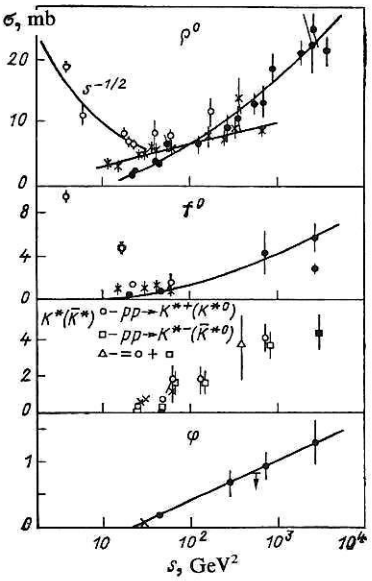

FIG. 7. Energy dependences of resonance production cross sections in pp (black circles). $p\bar{p}$ (open circles), and $\pi^{\pm} p$ (crosses) interactions. The curves are explained in the text (see Sec. 2).

high energies even for the lightest resonances (ρ^0 mesons).[7] Naturally, for the heavier meson and, especially, baryon resonances one must expect an increase in this transition point, which must be taken into account when the existing data are extrapolated to higher energies (for example, for the energies of the new CERN accelerator, $E \sim 150$ TeV).

The mean multiplicities $\langle n(R_i) \rangle$ in inelastic pp interactions are practically constant for $E \gtrsim 100$ GeV and are $\langle n(\rho^0) \rangle = 0.60 \pm 0.06$, $\langle n(f) \rangle = 0.17 \pm 0.03$, and $\langle n(K^*(890)) \rangle \approx 0.14 \pm 0.04$.[29] This is due to the fact that in the considered energy interval the total interaction cross sections of hadrons increase in the same way ($\sigma \sim \ln^2 s$) as $\sigma(R_i)$.

Knowing the cross sections $\sigma(R_i)$, we can find the fractions of the various species of long-lived particles produced by their decays. For example, for π^- mesons in pp collisions

$$\left.\begin{aligned} \alpha(\rho^0 \to \pi^-) &= \frac{\sigma(pp \to \rho^0 X)}{\sigma(pp \to \pi^- X)} = 0.13 \pm 0.01; \\ \alpha(f \to \pi^-) &= \frac{\sigma(pp \to fX)}{\sigma(pp \to \pi^- X)} = 0{,}025 \pm 0.005. \end{aligned}\right\} \qquad (22)$$

From this it is possible to estimate the total fraction of the negative secondary pions produced by the decays of the light meson resonances (ρ, ω). For this purpose, we use the data on $\sigma(\rho)$ and $\sigma(\omega)$ at $E = 10$–24 GeV.[5] They show that $\sigma(\rho^+) \approx \sigma(\rho^-) \approx \sigma(\rho^0)$ and $\sigma(\rho^0) \approx \sigma(\omega^0)$. Similar relations between the cross sections for the central region are obtained in quark models.[5,7,18] As a result, we obtain $\alpha_{\pi}(\rho, \omega) = 52\%$!

For more accurate determination of $\alpha(R_i)$, information is needed about $\sigma(R_i)$ for the various species of resonance. At relatively low energies ($E \lesssim 40$ GeV), such data are available. As an illustration, we give the values of $\sigma(R_i)$ in $\pi^+ p$ interactions at $p = 16$ GeV/c (see Table I).[21] It can be seen from the table that $51 \pm 4\%$ of the π^- mesons are produced by decays of identified meson resonances, among which about 43% give decays of vector mesons (ρ, ω). Similar results have also been obtained in other experiments for Kp, πp, $\bar{p}p$, and pp

interactions at $E \lesssim 40$ GeV.[5,7] At higher energies, because of the methodological problems in identifying the resonances (see Sec. 1), the information about $\sigma(R_i)$ is much sparser (Table II).[29] However, in this case too ($E \approx 1400$ GeV) we have $\alpha(\rho, \omega, f) \approx 60\%$. Thus, pions, which constitute the main fraction ($\approx 90\%$) of the secondary long-lived particles, are frequently produced by the decay of resonances and are therefore only indirectly related to the interaction dynamics of the primary hadrons.

The situation is similar for the K mesons. More than 50% of the K mesons are produced by the decays of the $K^*(890)$ resonances.[7,29,30]

It can also be seen from the data obtained at high energies (see Table II) that besides the vector mesons with a relatively large cross section the resonances f, $K^*(1430)$, and g with larger spins ($J^P = 2^+, 3^-$) are produced. Their production cross sections are about 20–25% of the cross sections of the corresponding vector mesons [ρ, $K^*(890)$], but in the decays they give, as a rule, more pions than the vector particles.[17] Therefore, their contribution to the production of pions and kaons is appreciable. Unfortunately, at high energies there are no more complete data on the production of resonances belonging to the higher unitary multiplets. At relatively low energies ($p = 32$ and 70 GeV/c), such information has been obtained for $K^\pm p$ interactions.[27] Table III gives data on the mean multiplicities of vector and tensor mesons in $K^\pm p$ interactions at $p = 32$ GeV/c. For comparison, we also give $\langle n(R_i)\rangle$ obtained in the framework of the additive quark model; these agree satisfactorily with experiment, except for $\langle n(K^\pm(890)\rangle$. The sum of the cross sections for the production of tensor (T) mesons [$K^*(1430)$, f] is $16 \pm 2\%$ of the total inelastic cross section of Kp interactions [$\sigma_{\text{inel}}(K^+p) = 15.33$ mb], whereas the cross section for vector (V) mesons is $66 \pm 4\%$ and R (T/V) ≈ 0.25. Thus, the tensor mesons may give about 20–25% of the secondary pions and kaons. Thus, the available data on the production cross sections of the meson resonances show that about 70–80% of the pions and kaons are produced as a result of their decays.

In contrast to the mesons, the secondary baryons are largely produced by the fragmentation of the primary nucleons ($N \to B$).[5,7,30,31] Indeed, the energies are still too low ($E \leqslant 2$ TeV) for copious production of baryon–antibaryon pairs [$n(\bar{p}) \lesssim 0.1$ and $\langle n(\bar{\Lambda}) \lesssim 0.01$ (Ref. 5)]. In this connection, the "threshold" effects in the energy dependence of $\sigma(R_i, s)$, which for light meson resonances appear at $E \lesssim 100$ GeV, are important in the entire region of the considered energies in the case of the baryons. Allowance for these effects is extremely complicated and model-dependent. For the fragmentation region, models such as the additive quark model give many helpful relations between $\sigma(R_i)$ (see Sec. 4).[18,32–35]

Information about production of baryon resonances is much sparser than it is about the meson resonances. This is due to the methodological difficulties of identifying broad nucleon resonances, the problem of identifying particles with $p \gtrsim 1$ GeV/c, and the small production cross sections of the strange resonances (see Sec. 1). At the present time, there are data on the production cross sections of the $\Delta^{++}(1232)$, $\Sigma^\pm(1385)$, and $\Xi^0(1530)$ resonances in $\pi^\pm p$, $K^\pm p$, and pp interactions at $E \lesssim 400$ GeV (Refs. 5, 7, 26–28, and 30). It has been established that about 30% of the protons, Λ particles, and Ξ hyperons are produced by decays of these resonances. For example, in $E = 405$-GeV pp interactions $28 \pm 4\%$ of the Λ^0 particles are produced in $\Sigma^{*\pm}(1385)$ decays.[30] At higher energies ($E = 1000$ GeV) in pp collisions there is found to be copious production of heavy nucleon isobars: $N^*(1520)$ and $N^*(1688)$ ($\sigma \approx 0.6$ mb).[31] Unfortunately, because of the methodological difficulties of identifying the production of baryon resonances in colliding-beam experiments, data on the total $\sigma(B_i^*)$ at $E \gtrsim 400$ GeV are almost absent.

Thus, it has now been established that for $E \gtrsim 100$ GeV a large fraction, 60–80%, of the secondary particles have a "resonance" origin. What is the source of the remainder? As yet, the methodological difficulties of identifying short-lived states at $E \gtrsim 100$ GeV make it impossible to answer this question definitively. There are only indirect arguments that the contribution of heavy resonances (or clusters) is also important.[4] Therefore, not more than 10% of the pions and kaons are directly produced in the primary collisions of the particles. This estimate of the fraction of "direct" pions follows from analysis of the distributions of the resonances and the pions with respect to their transverse momenta (see below). Another estimate was made in the framework of the additive quark model, which satisfactorily describes the experimental data on $\sigma(R_i)$.[18,33] It was found that the fraction of "direct" pions does not exceed 5% (see Sec. 4).

Distributions of Resonances with Respect to the c.m.s. Longitudinal and Transverse Momenta

In the region $E = 10$–30 GeV, the c.m.s. rapidity distributions of the ρ mesons have a plateau for $|y^*| \lesssim 1$ and decrease rapidly for $|y^*| \gtrsim 1$–1.5 for pp interactions.[5,7] To with-

TABLE II. Resonance-production cross sections in pp interactions at $\sqrt{s} = 52.5$ GeV ($p \approx 1460$ GeV/c).

Resonance	$\sigma(R_i)$, mb	$\frac{\sigma(R_i \to \pi^-)}{\sigma(pp \to \pi^-)}$, %
ρ^0	24.3±2.1	15±2
f^0	5.4±1.2	2.5±0.5
g^0	2.2±0.6	~0.4
$\overline{K}^{*0}$ (892)	4.3±1.0	1.6±0.4
$\overline{K}^{*0}$ (1430)	1.0±0.2	~0.3
φ	1.3±0.4	~0.1

TABLE III. Mean multiplicities of meson resonances in $K^{\pm}p$ interactions at $p = 32$ GeV/c.

Type of resonance	$\langle n(R_i)\rangle_{K^+p}$	$\langle n(R_i)\rangle_{K^-p}$	Additive quark model
K^+ (890)	0.23±0.01	—	0.34
K^- (890)	—	0.24±0.02	0.32
K^0 (890)	0.21±0.03	—	0.19
$\bar{K}^0$ (890)	—	0.21±0.02	0.18
ρ^0	0.22±0.02	0.24±0.04	0.25
φ	0.031±0.006	0.036±0.005	0.030
K^+ (1430)	0.050±0.016	—	0.070
$\bar{K}^-$ (1430)	—	0.054±0.014	0.066
K^0 (1430)	0.049±0.016	—	0.031
$\bar{K}^0$ (1430)	—	0.074±0.022	0.031
f (1270)	0.060±0.014	0.05±0.02	0.043

in the errors of ± 10%, the ρ^0, ρ^+, and ρ^- distributions do not differ. In principle, this behavior of $\sigma(y^*)$ corresponds to the ideas about the production of ρ mesons in the central region, although the energies are still low.

At higher energies ($E = 0.2$–2.0 TeV), there are only the first data on $\sigma_{\rho^0}(y)$, obtained for pp interactions.[23] They are shown in Fig. 8. In this case, the range of variation of y is already four units and one can see a rapid decrease in the cross section $\sigma(\rho^0)$ as $y \to y(p)$, i.e., in the region of proton fragmentation ($p \to \rho^0$). If it is assumed that the central region is $|y| \leqslant 2$, and the fragmentation region by $y(p) - y \leqslant 2$, then at $\sqrt{s} = 63$ GeV we obtain $\sigma_f(\rho^0) = 1.9 \pm 0.4$ mb and $\sigma_c(pp \to \rho^0) = 8.1 \pm 1.2$ mb. Similar results are obtained for $\sigma[K^{\pm}(890)]$ in pp interactions at $p = 405$ GeV/c: $\sigma_f[p \to K^*(890)] = 0.6 \pm 0.3$ mb and $\sigma_c[pp \to K^*(890)] = 7.1 \pm 1.4$ mb.[30] Thus, the cross section for the production of meson resonances (ρ, K^*) in the central region is appreciably greater than in the nucleon fragmentation region.

For $\pi^{\pm}p$ and $K^{\pm}p$ interactions in the fragmentation region [$\pi^{\pm} \to \rho^{\pm}(\rho^0)$ and $K^{\pm} \to K^{\pm}{}^*(K^{*0})$] the production cross sections of these resonances are comparable with the corresponding cross sections for their production in the central region, which is due to the similar quark composition of the $\pi(K)$ mesons and $\rho(K^*)$ resonances. The relations between σ_f and σ_c are considered in the additive quark model (see Sec. 4).[5,7]

The most complete data on the momentum distributions of different resonances have been obtained in Kp interactions with p of energy 32 and 70 GeV/c.[27] Figure 9 shows

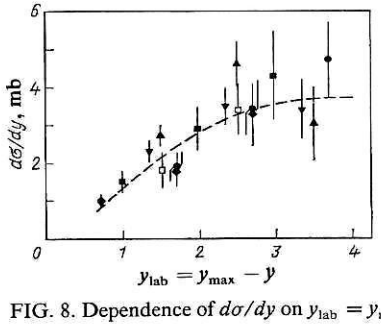

FIG. 8. Dependence of $d\sigma/dy$ on $y_{\text{lab}} = y_{\max} - y$ for $\sqrt{s} = 20$–63 GeV.

the invariant structure functions

$$f(x) = \int \left(\frac{E^*}{p^*_{\max}}\right) \frac{d^2\sigma}{dx\, dp_\perp^2} dp_\perp^2 \qquad (23)$$

for the $K^+(890)$, $K^+(1430)$, $K^0(890)$, and $K^0(1430)$ resonances produced in K^+p interactions at $p = 32$ GeV/c.[3)]

The diffraction and quasi-two-particle channels for production of resonances are eliminated from these distributions, and the scales of the cross sections along the ordinate are chosen to make the areas under the distributions $f(x)$ of the vector and tensor mesons equal. Figure 10 gives $d\sigma/dy^*$ for the ρ^0 and f^0 mesons, and $\sigma(\rho^0)$ normalized by $\sigma(f^0)$. From these distributions and Table III a number of important conclusions can be drawn.

First, the cross sections for the production of meson resonances belonging to one unitary multiplet are the same to within the errors, except for $\sigma(\varphi)$. For the multiplet of vector mesons [$K^*(890)$, ρ with $J^P = 1^-$], $\langle n(R_i)\rangle = 0.22 \pm 0.02$, and for the tensor mesons [$K^*(1430)$, $f(1270)$ with $J^P = 2^+$], $\langle n(R_i)\rangle = 0.056 \pm 0.018$. The coefficient of "suppression" of the production of the tensor mesons relative to the vector mesons is $\lambda = 0.25$. Hence and from other experiments (Ref. 5, 7, and 31–35) it follows that the cross sections for the production of resonances belonging to one unitary multiplet are approximately the same, while the probability for production of the tensor mesons is 0.25–0.30 that of the vector mesons.

Second, to within the errors the mean multiplicities of the resonances are the same in the K^+p and K^-p interactions at the same energy and for the corresponding substitution $K^+{}^* \to K^-{}^*$, $K^0{}^* \to \bar{K}^0{}^*$. This means that the strange and ordinary quarks in the primary K mesons [$K^+(\bar{s}u)$, $K^-(s\bar{u})$] fragment into hadrons independently of each other, and the probability of "coalescence" of the valence quarks of the K mesons and nucleons is small.[27]

In addition, the actual distributions of the structure functions with respect to x and y^* (see Figs. 9 and 10) do not differ, to within the errors, for resonances with the same quark composition [$f(K^*(890) \approx f(K^*(1430))$ and $f(\rho^0)$

[3)] At $p = 70$ GeV/c, $f(x)$ hardly differs from the functions given in Ref. 27.

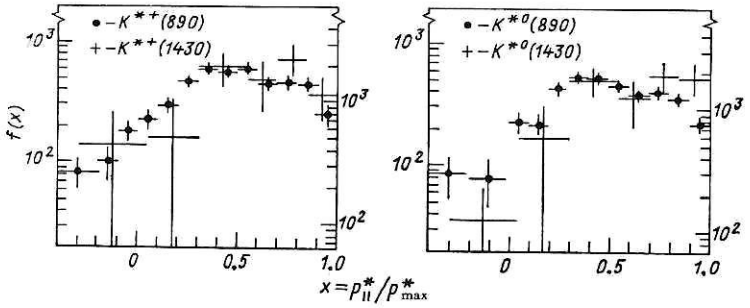

FIG. 9. Structure functions of K^* mesons produced in K^+p interactions at $p = 32$ GeV/c.

$\approx f(f^0)$].

In this connection, it is natural to assume that they have the same (or a universal) production mechanism. All these results confirm the basic assumptions of the additive quark model in the first approximation.[18,32–35]

The experimental information on baryon resonances is much sparser (see Sec. 1).

In Refs. 26 and 27, a study was made of the production of baryon resonances in the reactions

$$K^{\pm}p \to \Delta^{++}\ (1232) + X, \tag{24}$$

$$K^{\pm}p \to \Sigma^{+}\ (1385) + X, \tag{25}$$

$$K^{\pm}p \to \Sigma^{-}\ (1385) + X \tag{26}$$

at $p = 32$ and 70 GeV/c. The total cross sections $\sigma(R_i)$ and the momentum distributions of the resonances were obtained. For example, for K^+p interactions $\sigma(\Delta^{++}) = 1.77 \pm 0.16$ mb, $\sigma[\Sigma^+(1385)] = 0.119 \pm 0.020$ mb, and $\sigma[\Sigma^-(1385)] = 0.053 \pm 0.016$ mb. The distributions of the resonances with respect to x and y show that they are produced mainly in the proton fragmentation region. The basic features of these distributions with respect to x can be explained qualitatively by recombination of a valence diquark of the proton (uu) with u quarks from the "sea" for the Δ^{++} isobars; for $\Sigma^+(1385)$, besides this process, the mechanism of recombination of one of the valence u quarks is also important; $\Sigma^-(1385)$ is produced by the recombination of a valence d quark of the proton.[4)]

In the region of proton fragmentation ($x \leqslant -0.5$), where the diquark (uu) recombination mechanism is predominant, the spectra of the Δ^{++} and Σ^{*+} resonances have a similar shape, and the ratio of their cross sections is $\frac{\sigma(\Sigma^{*+})}{\sigma(\Delta^{++})} \approx 0.075$ [after subtraction of the contribution of diffraction dissociation to the cross section $\sigma(\Delta^{++})$], which agrees well with the prediction of the additive quark model.[27] Similar results were obtained in other experiments at $E \leqslant 400$ GeV.[34,35] These data show that at the existing energies, when the baryon resonances are largely produced in the nucleon fragmentation region, there are different mechanisms of their "formation" from the "primary" quarks. The relationship between them is as yet almost unknown, and therefore the theoretical interpretation of their production is much more complicated than for meson resonances (see Sec. 4).[34,35]

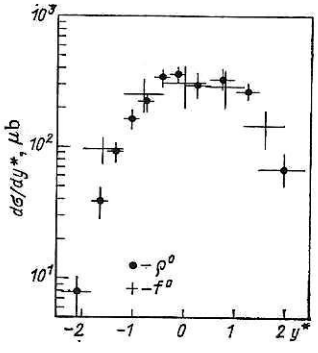

FIG. 10. Distributions of ρ^0 and f^0 mesons with respect to y^* (Kp interactions, $p = 32$ GeV/c).

Of special interest are the momentum distributions of the resonances and baryons in the fragmentation region of the primary particles ($|x| \geqslant 0.1$–0.5). It is expected in various theoretical approaches and on the basis of naive quark ideas that at high energies these momentum distributions reflect the distributions of the quarks in the primary hadrons.[7,36] In this connection, the invariant cross sections of hadron production are usually approximated by the function

$$f(x) = A\ (1 - |x|)^n, \tag{27}$$

which describes the structure functions of the valence quarks in the nucleons obtained from experiments on deep inelastic lepton–nucleon scattering. In Table IV, we give the values of n_{exp} obtained for K^+p interactions at $p = 32$ GeV/c.[37] The diffraction and quasi-two-particle channels in the processes $K^+p \to K^+(890), K^n X$ were eliminated. In the same table, we give the theoretical values (n_{th}) obtained on the basis of quantum chromodynamics.[38] In the model it is assumed that the distribution of the valence quarks varies weakly as a result of the primary interaction initiated by gluon exchange. The production of secondary hadrons in the fragmentation regions occurs as a result of recombination of one of the valence quarks (or a diquark) of the meson (or baryon) with sea quarks. The difference between the x distributions of the $\bar{s}$ and u quarks in the primary K mesons was not taken into account. As can be seen from Table IV, there is good agreement in the nucleon fragmentation region ($x \leqslant -0.3$) between n_{exp} and n_{th}. The x distributions for π^+ and π^- mesons in the nucleon fragmentation region agree with the x distributions of the corresponding u and d quarks in the proton known from deep inelastic lepton–nucleon

[4)]We recall the quark composition of the baryon resonances: $\Delta^{++}(uuu)$, $\Sigma^{+*}(uu\bar{s})$, $\Sigma^{-*}(dds)$.

TABLE IV. Values of n_{exp} obtained by approximating $f(x)$ by the function (27) for K^+p interactions at $p = 32$ GeV/c.*

Type of particle	Interval of x	n_{exp}(32 GeV/c)	n_{th}
K^-n	$\geqslant 0.3$	0.60 ± 0.05	1
K^{*+} (890)	$\geqslant 0.3$	0.30 ± 0.06	1
π^-	$\geqslant 0.6$	2.1 ± 0.1	3
ρ^0	$\geqslant 0.3$	2.1 ± 0.5	1
$\bar{\Lambda}^0$	$\geqslant 0.3$	1.60 ± 0.15	2
Λ^0	$\leqslant -0.5$	1.0 ± 0.2	1
Σ^{*+} (1385)	$\leqslant 0$	$\ll 1$	1
Σ^{*-} (1385)	$\leqslant 0$	1.8 ± 0.7	4
ρ^0	$\leqslant -0.3$	3.1 ± 0.4	3
π^+	$\leqslant -0.6$	3.0 ± 0.2	3
π^-	$\leqslant -0.6$	3.9 ± 0.7	4

*Similar results for n_{exp} are obtained for K^+p (70 GeV/c) and K^-p (110 GeV/c) interactions.

scattering [$u(x)\sim(1-x)^3$ and $d(x)\sim(1-x)^4$]. On the other hand, there is an appreciable discrepancy for the kaon fragmentation region ($x\geqslant 0.3$). In Ref. 37 it is attributed to the difference between the x distributions of the s and u quarks in the primary $K^\pm$ mesons. Indeed, the difference between the momentum distributions of the ρ and f mesons and the K^* resonances (see Figs. 9 and 10) shows that $f(x)$ for the u quarks (ρ and f mesons) is not the same as for the s quarks (K^* resonances). These data were used to obtain the estimates $\langle x(\bar{s})\rangle = 0.35$ and $\langle s(u)\rangle = 0.17$, where $\langle x(\bar{s}, u)\rangle$ are the mean fractions of the total reduced momentum of the primary kaon corresponding to the valence quarks.[39]

At higher energies ($E = 0.1$–2 TeV), there are as yet unfortunately no such complete data on $f(x)$ for resonances. In this connection, it is generally the distributions of the secondary baryons, which are frequently produced directly, that are analyzed. For example, for pp interactions ($\sqrt{s} = 25$–62 GeV) approximation of the baryon distributions by the function (27) in the region $x = 0.2$–0.8 yielded the following values[40]: $n(\bar{\Lambda}, \bar{p})\approx 5$, $n(\Sigma^-)\approx 3$, $n(\Sigma^+, \Lambda^0)\approx 1$ and $n(p)\approx -1$. These values of n correspond to the n_{th} obtained from quark counting rules[41]: $n_i = 2n_q - 1$, where n_q is the number of different quarks in the primary and the secondary baryon, and they do not contradict the results obtained in Kp interactions (see Table IV).

Thus, the first data on $f(x)$ for the resonances and baryons show that at large values of $|x|$ they probably reflect well the quark distributions in the primary hadrons. However, the errors in the determination of $n_{ex}(R_i)$ are still large (especially as $|x|\to 1$) and the energy is too low for one to be able to identify unambiguously the fragmentation region. Therefore, measurements of $f(x)$ for resonances at $E\geqslant 1$ TeV are needed.

Interesting results are obtained when the distributions of the resonances with respect to their transverse momenta are analyzed.[5,7] Already at low energies ($E\lesssim 30$ GeV) it was noted that these distributions of resonances with $M\lesssim 1.4$ GeV [ρ, ω, η, f, $K^*(890)$ and the Δ, $\Sigma^*(1385)$ baryons produced in πp, Kp, $p\bar{p}$, and pp interactions] can be well described by the simple dependence.

$$\frac{1}{\sigma(R_i)}\frac{d\sigma}{dp_\perp^2} = \langle n(R_i)\rangle \exp(-bp_\perp^2) \tag{28}$$

with $\langle b\rangle \approx 3.4\,(\text{GeV}/c)^{-2}$ in the range of variation of $p_\perp^2$ from 0.2 to 2 $(\text{GeV}/c)^2$.[5] The difference between the values of b for the different resonances does not exceed 10%. This means that $\langle p_\perp(R_i)\rangle = 0.5$ GeV/c (for pions, $\langle p_\perp\rangle \approx 0.34$ GeV/c). At higher energies ($\sqrt{s} = 23$–63 GeV) it was found for ρ^0 mesons produced in pp interactions that $b = 3.3 \pm 0.2$ $(\text{GeV}/c)^{-2}$ and $\langle p_\perp(\rho^0)\rangle = 0.49 \pm 0.02$ GeV/c (Ref. 23).[5)]

The universality of the distributions of the resonances with respect to $p_\perp^2$ makes it possible to estimate the fraction of "direct" pions.[5] It is found that for $p_\perp \geqslant 1$ GeV/c the pion distribution can also be described by (28) with $b\approx 3.4$ $(\text{GeV}/c)^{-2}$, whereas at smaller $p_\perp$ it has a complicated form (Fig. 11). A natural explanation of this phenomenon is that the overwhelming majority of the pions with $p_\perp \lesssim 1$ GeV/c are produced by the decay of resonances. The lower the energy release in the decay of the resonances, the smaller the transverse momentum of the decay ions. Therefore, the distribution of all the pions differs strongly from (28). On the other hand, the similar behavior of the pions and the resonances for $p_\perp \geqslant 1$ GeV/c suggests that they are all produced in the same way. Hence, by extrapolation to $p_\perp^2 \to 0$ in accordance with Eq. (28) it was found that the fraction of direct pions is $\alpha(\pi_d)\approx 10\%$.[5,21]

A different estimate of the fraction of direct pions (about 5%) was obtained in the framework of the additive quark model with allowance for the experimental data on the production of some heavy meson resonances [f, $K(1420)$, g].[33] A similar treatment of the production of kaons in pp interactions at $p = 405$ GeV/c shows that the fraction of the "direct" kaons does not exceed 30%.[30]

Of course, for a model-independent quantitative estimate of $\alpha(\pi_d)$ and $\alpha(K_d)$ we need experimental data on the production of heavy resonances (or clusters). However, the available results do indicate that the overwhelming majority

[5)]The value of $\langle p_\perp(R_i)\rangle$ is larger for heavier resonances. For example, for the ψ mesons $\langle p_\perp\rangle = 1.29 \pm 0.05$ GeV/c and for Υ we have $\langle p_\perp\rangle = 1.75 \pm 0.19$ GeV/c at $\sqrt{s} = 63$ GeV.[29] A certain increase in $\langle p_\perp(R_i)\rangle$ for $K^*(890)$ with increasing energy is also observed.[27]

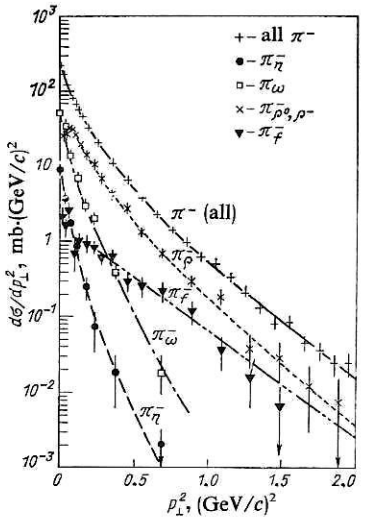

FIG. 11. Distributions of pions from the decays of ρ, f, η, and ω mesons with respect to $p_\perp^2$ ($\pi^+ p$ interaction at $p = 16$ GeV/c).

of the pions and kaons are produced by the decay of resonances. This leads to a review of the nature of the behavior established for the production of long-lived particles.[5,7] Most of the behavior is determined not by the interaction dynamics but by the kinematics of resonance decays, which is known from experiments at low energies ($E \lesssim 10$ GeV).

Characteristic examples here are the "seagull" effect [the increase in $\langle p_\perp(x)\rangle$ with increasing x for pions and kaons] and the increase in $\langle p_\perp(M)\rangle$ from 0.34 GeV/c for pions to 0.5–0.6 GeV/c for the Λ and Σ particles.[5,7] They can be readily explained by the established features of the production of resonances and direct pions and kaons ($\langle p_\perp\rangle \approx 0.5$ GeV/c). Therefore, in the first approximation there is no dependence of $\langle p_\perp\rangle$ on x and M in the first stage of the process (2). In the decays of the resonances, the transverse momenta of the pions and kaons decrease compared with $\langle p_\perp(R_i)\rangle$, this occurring more strongly the smaller the energy release (Fig. 11). It is at this stage of the process that the dependences $\langle p_\perp(x)\rangle$ and $\langle p_\perp(M)\rangle$ appear that were previously attributed to the interaction dynamics of the primary hadrons. The first direct experimental data for proton energy 32 and 70 GeV/c in the study of $\langle p_\perp(x)\rangle$ for the $K^*(890)$ resonances and their decay particles (π, K) confirm this conclusion (Ref. 27).[6)]

A more detailed analysis of the available data on the long-lived particles (π, K, N) produced in hadron collisions in the interval of energies from 5 to 1500 GeV made with allowance for the production of resonances showed that most of the properties of the single-particle inclusive distributions and the correlation functions of these particles can be explained by the resonance-decay kinematics.[42] Therefore, at the present time the main task of the experiments is to identify secondary short-lived states (resonances and clusters) as more direct sources of information about the structure of hadrons and the dynamics of the strong interactions.

[6)] K^+p interactions at $p = 32$ GeV/c: $\langle p_\perp[K^*(8901)]\rangle = 0.51 \pm 0.10$, $\langle p_\perp(K_S^0)\rangle = 0.44 \pm 0.02$, and $\langle p_\perp(\pi^-)\rangle = 0.34$ GeV/c.[27]

Polarization Characteristics of Secondary Baryons and Resonances

It is well known that at low energies the production cross section of secondary particles depends strongly on the direction of their spins, and therefore vector mesons are, as a rule, produced with alignment, and baryons are polarized. Measurement of their polarization characteristics gives important information about strong-interaction dynamics. At high energies, when many particles are produced and there is an averaging over the different mechanisms of their production (inclusive processes) it was expected that the secondary particles would be unpolarized. However, the first experimental data on this question show that at high energies too spin effects play an important part (Refs. 7, 27, and 43–47).

We begin the discussion of the data with the polarization of Λ^0 ($\bar\Lambda^0$) hyperons,[43–45] which are largely (about 70%) produced directly in the hadron interactions (see above). The separation of the secondary Λ ($\bar\Lambda$) particles gives problems associated with their identification and the large background of conversion e^+e^- pairs (see Sec. 1).[45] However, for $E \lesssim 400$ GeV the uncertainties in the identification of the Λ particles do not exceed 10%, and it was therefore possible to measure their polarization (**P**) in almost the entire range of the variable x.[43–45] The polarization of Λ hyperons was studied in the processes

$$h + p\ (n) \to \Lambda\ (\bar\Lambda) + X \to p\ (\bar p) + \pi^-\ (\pi^+) + X \qquad (29)$$

at $E \lesssim 1500$ GeV (h equal to π, K, N). In none of the experiments were the Λ ($\bar\Lambda$) particles from the decays $\Sigma^0 \to \Lambda\gamma$ and $\bar\Sigma^0 \to \bar\Lambda\gamma$ distinguished. In this case,

$$\mathbf{P}\ (\Lambda) = -1/3\mathbf{P}\ (\Sigma^0) \text{ and } \mathbf{P}\ (\bar\Lambda) = -1/3\mathbf{P}\ (\bar\Sigma^0),$$

and therefore the measured polarization of the secondary hyperons is less than the initial polarization. The relationship between the Λ and Σ production cross sections is, as a rule, unknown, and the influence of the depolarization effect is sometimes estimated on the basis of model assumptions about $\sigma(\Lambda)$ and $\sigma(\Sigma)$.

The polarization of the Λ ($\bar\Lambda$) hyperons is measured using the characteristics of the angular distribution of the protons (or antiprotons) in the rest frame of the hyperons:

$$f_N(\cos\theta) = a\,(1 + \alpha P \cos\theta_N), \qquad (30)$$

where θ_N is the angle between the momentum of the proton (or antiproton) and the normal to the hyperon production plane, and $\alpha(\Lambda) = 0.642$ [$\alpha(\bar\Lambda) = -0.642$] is the decay parameter. It follows from (30) that

$$\alpha P = \frac{\langle\cos\theta_N\rangle}{\langle\cos^2\theta_N\rangle}. \qquad (31)$$

Because of parity conservation in strong and electromagnetic interactions, the other projections of **P** vanish.

The most complete data on $P(\Lambda)$ and $P(\bar\Lambda)$ were obtained in $K^\pm p$ interactions in the range of momenta from 4 to 70 GeV/c.[27,44] For example, for K^+p interactions at $p = 70$ GeV/c,[44] the event statistics was 1152 with Λ particles and 518 with $\bar\Lambda$ particles [$\sigma(\Lambda) = 1.09 \pm 0.05$ mb and $\sigma(\bar\Lambda) = 0.65 \pm 0.04$ mb]. The mean values of the polarization over the complete range of x were $P(\Lambda) = 0.10 \pm 0.05$ and $P(\bar\Lambda) = -0.18 \pm 0.07$. A large polarization of the $\bar\Lambda$ particles was found for $x \geqslant 0.2$ [$P(\bar\Lambda) = -0.5 \pm 0.1$, i.e., in the

region of K^+ fragmentation. In this case, the primary K^+ meson [$K^+(\bar{s}u)$] and the $\bar{\Lambda}$ hyperon [$\bar{\Lambda}(\bar{u}\bar{d}\bar{s})$] have a common strange antiquark ($\bar{s}$). Similar results for $P(\Lambda)$ and $P(\bar{\Lambda})$ were obtained in $K^\pm p$ interactions at $p = 32$ GeV/c.[7,27,44]

The situation is somewhat different in NN and πN interactions (see the references in Refs. 43 and 45). In this case, the Λ polarization was studied mainly in the fragmentation region of the nucleons, but as a function of their transverse momentum [$p_\perp(\Lambda)$] (Fig. 12). For $\pi^- p$ interactions at $p = 40$ GeV/c,[43] the available data can be satisfactorily described by the expression

$$P(\Lambda) = (0.058 \pm 0.13) - (0.57 \pm 0.23)\, p_\perp(\Lambda) \quad (32)$$

and $\langle P(\Lambda)\rangle = -0.22 \pm 0.07$ ($p_\perp$ measured in GeV/c).

Thus, although the errors in the measurement of $P(\Lambda)$ are still large, overall the data obtained in different experiments and in a wide range of energies ($E = 10$–1500 GeV) show that there is an appreciable polarization of hyperons produced either in hard collisions ($p_\perp \gtrsim 1$ GeV/c) or in the fragmentation region of the primary particles.

The data on the polarization characteristics of meson resonances have been obtained only at relatively low energies ($E \lesssim 100$ GeV). They have been studied on the basis of the angular distributions of their decay products ($\rho \to \pi\pi$, $K^* \to K\pi$).

In pp interactions at $p = 24$ GeV/c, measurements were made of the elements of the spin density matrix (ρ_{ik}) for ρ^0 mesons.[46] It was found that $\rho_{00} = 0.34 \pm 0.06$, i.e., the production of ρ^0 mesons does not depend on the orientation of their spin ($\rho_{00} = 1/3$). We recall that in $pp \to R_i X$ processes the meson resonances are produced mainly in the central region, where the particle multiplicity is relatively large (see above). In $\bar{p}p$ interactions at $p = 22.4$ GeV/c an alignment ($\rho_{00} = 0.61 \pm 0.06$) of the ρ^0 mesons was found; this is attributed to the annihilation channels and must therefore decrease with increasing energy.[47]

In $K^\pm p$ interactions ($p \leqslant 70$ GeV/c), polarization effects were studied in the K fragmentation region [$x(K^*) = 0.4$–0.7] in the production of $K^*(890)$.[27] In this case, the background processes are unimportant and ρ_{ik} can be measured. It was found that pion exchange between the primary kaons and the protons makes an important contribution to the $K^*(890)$ production. Therefore, the resonances are produced aligned with respect to $\mathbf{p}(K^\pm)$.

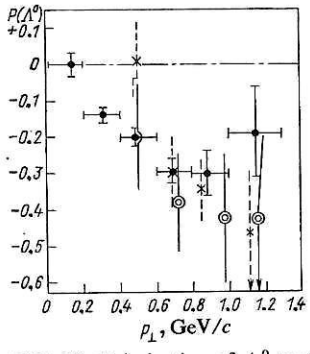

FIG. 12. Polarization of Λ^0 particles as a function of their transverse momentum. The black circles represent diffraction nC interactions ($\langle E_n\rangle = 40$ GeV); the crosses, pp interactions at $\sqrt{s} = 53$ GeV; and the double open circles, pp interactions at $\sqrt{s} = 62$ GeV.

Thus, the first experiments investigating spin effects in the production of resonances and baryons at high energies showed that they are important in the fragmentation regions of the primary particles. In the majority of quark models,[32–34,36] they are not taken into account (see Sec. 4). In quantum chromodynamics they are also absent in the first approximation. Therefore, measurement of the polarization characteristics of the secondary hadrons and resonances at high energies has fundamental importance for the development of both the theory of strong interactions and models. First attempts at their explanation are associated with subtle effects such as the polarization of the quarks (see the literature quoted in Ref. 43).

In this connection, a whole series of experiments is currently being planned with polarized beams and targets of primary particles in both lepton–hadron and hadron–hadron interactions at high energies.

3. PRODUCTION OF HADRONS IN HARD AND DEEP INELASTIC PARTICLE INTERACTIONS

In soft hadron collisions, the transverse momenta of the secondary particles are characteristically $\langle p_\perp(R_i)\rangle \approx 0.5$ GeV/c (see Sec. 2). Therefore, in these processes one is studying the structure of the hadrons and their interactions at relatively large distances ($r \gtrsim 0.2$–0.4 F). To investigate short distances ($r \lesssim 0.1$ F), it is necessary to go over to processes with large momentum transfers ($\Delta p \gtrsim 1$ GeV/c). In strong interactions, they have become known as hard collisions of hardons; in weak and electromagnetic interactions, as deep inelastic interactions.[1,2] In both cases, the interaction of the particles is regarded as due to the interaction of partons with partons (strong interactions) or with leptons (weak and electromagnetic interactions). After the interaction, the scattered partons (quarks and gluons) fragment into hadrons, and these are detected experimentally. From the point of view of the production of resonances (the final stage of the processes), these interactions have much in common, and they are therefore better considered together.

Hard Collisions of Hadrons

The production of secondary particles with $p_\perp \geqslant 1$ GeV/c in hadron collisions at high energies ($E \lesssim 2$ TeV) has now been studied intensively for more than a decade with all the largest accelerators in the world (Refs. 2, 10, 12, and 48). Much information has been obtained on the production cross sections and characteristics of the hadrons (or hadron jets). The theoretical interpretation of these processes is given in the framework of the quark–parton model with allowance for QCD effects.[2,12,48] The hard collision processes

$$h_1 + h_2 \to \Sigma h_i^{(1)} + \Sigma h_j^{(2)} + X \quad (33)$$

take place in several stages. First, the quarks (q_1, q_2) of the primary hadrons are scattered through large angles,

$$q_1 + q_2 \to q_1' + q_2', \quad (34)$$

and they then go over into hadrons,

$$q_{1,2}' \to \Sigma h_i^{(1)} + \Sigma h_j^{(2)}, \quad (35)$$

which, in their turn, decay into long-lived hadrons—which are then detected experimentally.

The subject of the present review is the final stage of the process (33): $q \to \Sigma h_i$. Therefore, we shall not discuss the problems associated with the behavior of the cross sections of the reactions (33) as functions of s and $p_\perp$ or the questions of identifying hadron jets.[12,48] However, we note that, taken together, the data on (33) show that the quark–quark scattering (34) is predominant for $p_\perp(q) \gtrsim 4$ GeV/c.[12,48] At smaller transverse momenta, other elementary processes of hard scattering in QCD with gluon participation may be important:

$$q + \bar{q} \to g + g, \tag{36}$$
$$q + g \to q + g, \tag{37}$$
$$g + g \to g + g, \tag{38}$$

with subsequent fragmentation $g \to \Sigma h_i$. These "background" processes complicate the comparison of data on hard and deep inelastic processes, because the hadrons in the latter are, as a rule, produced by quark fragmentation ($q \to \Sigma h_i$).

The multiplicity of the hadrons in jets with large transverse momenta is high ($n_{\text{ch}} \approx 5$–8), and therefore the identification of resonances on the basis of decays into pions and nucleons gives rise to the same methodological problems as in soft collisions. The CERN colliding proton beams have been used to study the production of neutral meson resonances on the basis of their decays into photons and e^+e^- pairs[49–51]:

$$p + p \to \pi^0\,(\eta^0,\ \omega^0,\ \eta') + X \to \gamma_1 + \gamma_2 + \gamma_3 + X, \tag{39}$$
$$p + p \to \rho^0\,(\varphi) + X \to e^+ + e^- + X. \tag{40}$$

The processes (39) were studied experimentally using four calorimeters (liquid argon counters with lead plates), which detected the photons in a solid angle of ≈ 3 sr at $\langle\theta\rangle \approx 90°$ relative to the proton collision axis.[49,50] The mesons were detected through the decays

$$\pi^0,\ \eta^0,\ \eta' \to 2\gamma,\ \omega \to \pi^0\gamma \to 3\gamma. \tag{41}$$

The emission angles of the photons and their energies were measured. The resolution with respect to the photon energy was $\sigma(E) = 10\%/\sqrt{E_\gamma}$, and the spatial resolution was $\sigma(x) \approx 5$ mm. The total calorimeter thickness was ≈ 18 radiation units, and therefore the γ detection efficiency was $\varepsilon \approx 100\%$. These characteristics of the calorimeters made it possible to achieve good separation of the signals from the pions and resonances ($r \gtrsim 1$) on the basis of a standard analysis of the spectra of the effective masses $M(\gamma\gamma)$, $M(\gamma\gamma\gamma)$, and $M(\pi^0\gamma)$ (Fig. 13). The result was the determination of $\sigma(R_i)$ and their branching ratios $[R(R_i/\pi^0) = \sigma(R_i)/\sigma(\pi^0)]$ at energies $\sqrt{s}$ equal to 53 and 63 GeV (Table V). It can be seen that in hard collisions too the production of resonances is clearly dominant. We recall that for soft interactions $R(\frac{\rho^0}{\pi^-}) \approx R(\frac{\omega}{\pi^-}) = 0.13$, while $R(\frac{\rho^0}{\pi^-}) \approx R(\frac{\omega}{\pi^-}) \approx 0.5 - 1.0$ for the region $p_\perp(R) = 1$–2 GeV/c (see Sec. 2).

In the processes (40), e^+e^- pairs were detected with $M(e^+e^-) = 0.52$–1.2 GeV/c^2 and $p_\perp(e^+e^-) \geqslant 1.8$ GeV/c.[51] Values were obtained for $R(\rho^0/\pi^0)$ and $R(\varphi/\pi^0)$ for

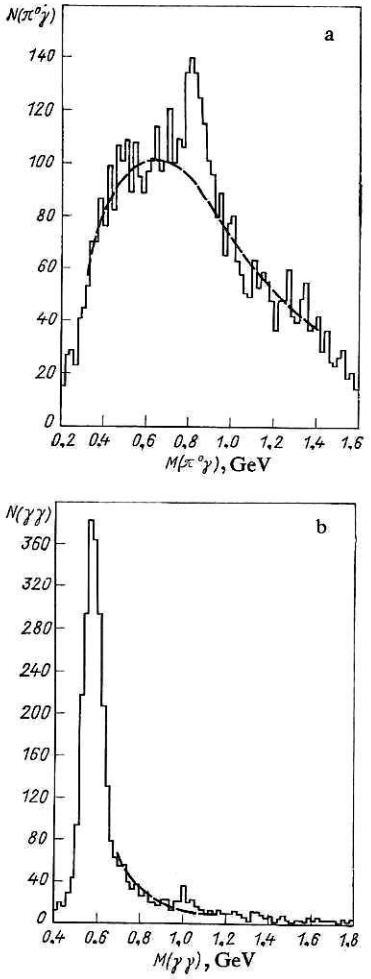

FIG. 13. Effective-mass spectrum of the $\pi^0\gamma$ and $\gamma\gamma$ systems produced in pp interactions at $p_\perp \geqslant 6$ GeV/c, $x = 0$, and $\sqrt{s} = 53$ GeV. The broken curve is the background.

$\langle p_\perp \rangle = 2.2$ GeV/c (Table V).

There are also individual data on the production of other resonances obtained by studying their decays into pions, kaons, and protons.[48] In this case, resonance production was studied in the so-called trigger hadron jet, in which, as a rule, there are few particles ($n_{\text{ch}} = 2$–3) and one particle has a large transverse momentum. The trigger particles (h_{tr}) were taken to be $\pi^\pm$ and $K^\pm$ mesons, protons, and antiprotons with $p_\perp = 2$–3 GeV/c produced in pp interactions at $\sqrt{s} = 31.53$ GeV and $\theta = 90°$. The distributions with respect to the effective masses of the particles in the trigger jet were then constructed. The event statistics was not large, and it was found that[48]

$$R\left(\frac{\rho^0}{\pi^-_{\text{tr}}}\right) \approx 1,\ R\left(\frac{K^*(890)}{K^-_{\text{tr}}}\right) \gtrsim 1 \text{ и } R\left(\frac{\Delta^{++}}{P_{\text{tr}}}\right) > 1.$$

Unfortunately, more complete data on $\sigma(R_i)$ are as yet unavailable. Nor are there distributions of the resonances over x, y, and $p_\perp$ relative to the axis of the hadron jet. Nevertheless, these results already show that the fraction of resonances among the secondaries is large and, probably, not less than in soft hadron collisions (see Sec. 2). Therefore, in theoretical models describing hard hadron collisions it is, as a

TABLE V. Relative yields of meson resonances at large $p_\perp(R)$ in pp interactions ($\sqrt{s} = 53$ and 63 GeV).*

Type of resonance	Interval of $p_\perp(R)$, GeV/c	Values of $\langle R_i\rangle/\langle\pi^0\rangle$
$R\ (\omega/\pi^0)$	3–7	0.87 ± 0.17
$R\ (\eta/\pi^0)$	3–11	0.55 ± 0.07
$R\ (\eta'/\pi^0)$	3–7	0.90 ± 0.25
$R\ (\rho^0/\pi^0)$	2.2	0.58 ± 0.19
$R\ (\varphi/\pi^0)$	2.2	0.12 ± 0.05

*The values of $\langle R_i\rangle/\langle\pi^0\rangle$ do not depend on $\sqrt{s}$ and $p_\perp(R)$.

rule, assumed that there is intensive production of resonances when quarks fragment into hadrons in accordance with (35).[2,12,35] For example, in the popular Field-Feynman model,[2] which is widely used for comparison with experiment, $\alpha(\mathrm{P}) = \alpha(\mathrm{V})$ and $\alpha(\mathrm{T}) = 0$ ($\alpha_i(R_i)$ are the fractions of pseudoscalar (P), vector (V), and tensor (T) mesons in the fragmentation $q \to \Sigma h_i$). These values of $\alpha(R_i)$ were taken from the first experiments[48] on $\sigma(R_i)$. They are free parameters of the model.

As yet, there are no data on the momentum distributions of the resonances and the quark fragmentation processes in strong, weak, and electromagnetic interactions are compared on the basis of the characteristics of the long-lived hadrons. We shall give them below; here, we briefly list some of them for pp interactions at $\sqrt{s} = 31$–63 GeV for $\theta^* = 90°$ (Refs. 5, 4, 8, and 12).

1. As $p_\perp$ increases from 0.3 to 4 GeV/c, the fraction of $\pi^\pm$ mesons among the charged secondaries decreases from 0.9 to 0.55 ± 0.05, while the fraction of heavy particles increases: $K^\pm$ from 0.07 to 0.27 ± 0.04, $\bar{p}$ from 0.02 to 0.07 ± 0.02 and p from 0.04 to 0.12 ± 0.02. A similar phenomenon is observed in e^+e^- annihilation.

2. The distributions of the secondary hadrons with respect to their transverse momenta relative to the jet axis are bounded ($\langle p_\perp\rangle \approx 0.5$ GeV/c) and recall the analogous distributions for soft hadron collisions. They do not depend (or depend weakly) on the transverse momentum of the jet (J) of hadrons for $p_\perp(J) = 2$–7 GeV/c.

3. The distributions of the hadrons with respect to $x_\parallel = p_\parallel/p(J)$, where $p_\parallel$ is the longitudinal momentum relative to the hadron-jet momentum ($p(J)$), do not depend on $p(J)$ for $p_\perp(J) \gtrsim 3$ GeV/c and $x_\parallel \gtrsim 0.1$.

4. Short-range correlations have been found[2,12,48] between the particles of a jet, these being similar to the correlations between the hadrons in soft collisions.[5–7] For differently charged particles they are much stronger than for hadrons of the same charge sign. This last result clearly indicates copious resonance production.

5. The transverse momenta of the quarks (q_1, q_2) in the primary hadrons are large and reach $k_\perp \approx 0.8$–1 GeV/c at large $p_\perp(h)$, which is very important for the correct identification of the hadron jets and the determination of their characteristics in hard hadron collisions.[2,12,48] A more detailed description of the main features of the processes of quark fragementation into hadrons in hard collisions can be found in the reviews of Refs. 2, 5, 12, and 48.

Deep Inelastic Lepton–Nucleon Interactions

In recent years, there has been intensive study of the production of hadrons in deep inelastic lepton–nucleon interactions[13,52–54]:

$$lN \to l + q_i \to \gamma^*(W) + q_i \to q_j + X \to \Sigma h_j + X, \quad (42)$$

in which the quarks subsequently fragment into hadrons in accordance with (35). Here, l are leptons ($e, \mu, \nu, \bar{\nu}$) and $\gamma^*(W)$ are virtual photons (intermediate vector bosons) emitted by the leptons. The cross section of the processes (42) can be expressed in terms of the distribution functions of the quarks in the nucleons. $F_q^N(x', k_\perp^2)$, and the functions describing the fragmentation of the quarks into hadrons, $D_q^h(x, p_\perp^2)$, where x' (x) are the fractions of the momentum of the quarks (respectively, hadrons) in the total momentum of the nucleons (quarks) (Refs. 1, 12, 13, and 52–54).[7)] The determination of the structure functions of the quarks in the nucleons ($F_q^N(x', k_\perp^2)$) from data on the cross sections of the processes (42) and their comparison with the predictions of QCD and the quark–parton models is one of the brilliant chapters of high-energy physics and has been studied in detail in many reviews (see, for example, Refs. 1, 2, 12, 13, and 52–54).

The fraction of the nucleon momentum carried away by all quarks ($q + \bar{q}$) is 0.45 ± 0.01, by valence quarks ($q + \bar{q}$) it is 0.32 ± 0.01, and by sea quarks ($q\bar{q}$) it is 0.13 ± 0.01. It follows from this that about 50% of the nucleon momentum is "carried" by the gluons. The actual distributions of the quarks in the nucleon with respect to x' are shown in Fig. 14, from which it can be seen that for $x' \gtrsim 0.2$ sea quarks are

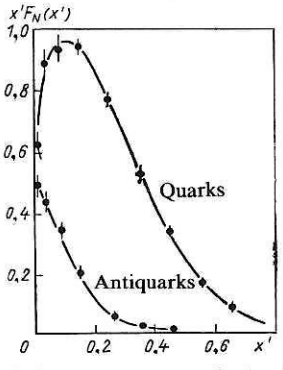

FIG. 14. Momentum distributions of quarks and antiquarks in the nucleon.

7)Here, we shall denote the Feynman variable $x = p_\parallel^*/p_{\parallel\max}$ by x_F, to distinguish it from x (x').

virtually absent.

Table V gives the quark composition that has the preferred fragmentation in the region of primary particles for different deep inelastic interactions. For weak interactions, it is determined by the charge conservation law:

$$\nu\,(\bar{\nu}) + p\,(uud) \to W^+\,(W^-)$$
$$d\,(u) \to u\,(d) + uu(ud) + \mu^-\,(\mu^+), \qquad (43)$$

and for electromagnetic interactions by e_q^2. The estimates show that this quark composition determines about 8/9 of the cross section for charged leptons and about 90% of the cross section for neutrino interactions, Thus, deep inelastic lepton–hadron interactions make it possible, in principle, to study the fragmentation of the individual species of quarks and diquarks (Table VI).

We turn to a discussion of the experimental data.[52–63] The results obtained in the first experiments and the method are considered in the reviews of Ref. 13. Data on the production of resonances in weak interactions with charged currents.

$$\bar{\nu}\,(\nu) + p \to \mu^+\,(\mu^-) + R_i + X, \qquad (44)$$

are mainly obtained using large bubble chambers (5 m) exposed to ν and $\bar{\nu}$ beams with $E = 10$–200 GeV in the accelerators at CERN and Batavia. In the experiments of Refs. 55 and 56, 2289 $\bar{\nu}$ events and 7831 ν events were detected. The mean characteristics of the selected events were $\langle E_{\bar{\nu}}\rangle = 31$ GeV, $\langle W\rangle = 3.4$ GeV, $\langle Q^2\rangle = 2.7\,(\text{GeV}/c)^2$ for the $\bar{\nu}$ experiment[55] and $\langle E_\nu\rangle = 40$ GeV, $\langle W\rangle = 4.4$ GeV, and $\langle Q^2\rangle = 6.4\,(\text{GeV}/c)^2$ for the νp interactions.[56]

Here, W is the total energy of the hadrons in their c.m.s.:

$$W^2 = M^2 + 2M\,(E_{\nu(\bar{\nu})} - E_\mu) - Q^2, \qquad (45)$$

Q is the momentum transfer,

$$Q^2 = (P_{\nu(\bar{\nu})} - P_\mu)^2 = (E_{\nu(\bar{\nu})} - E_\mu)^2 - (\mathbf{p}_{\nu(\bar{\nu})} - \mathbf{p}_\mu)^2, \qquad (46)$$

and $E_{\nu(\bar{\nu})}, E_\mu, \mathbf{p}_{\nu(\bar{\nu})}, \mathbf{p}_\mu$ are the energies and momenta of the leptons and M is the mass of the nucleons. The secondary charged particles were identified by means of their ionization for $p \lesssim 1$ GeV/c; at larger momenta, they were assumed to be pions. Figure 15 shows the distributions of $M(\pi^+\pi^-)$ and $M(\pi^\pm\pi^\pm)$ for $\bar{\nu}p$ interactions.[55]

A ρ^0-meson signal can be seen in the $M(\pi^+\pi^-)$ distribution but not in the $M(\pi^\pm\pi^\pm)$. These data were analyzed in accordance with the standard procedure (see Sec. 1) and it

TABLE VI. Species of fragmenting quarks in different interactions.

Type of interaction	Fragmentation	
	of target	of beam
νp	(uu)	u
$\bar{\nu}p$	(ud)	d
l^+p	(ud)	u
e^+e^-	—	$q\,(\bar{q})$
hN	(qq)	$q\,(\bar{q})$

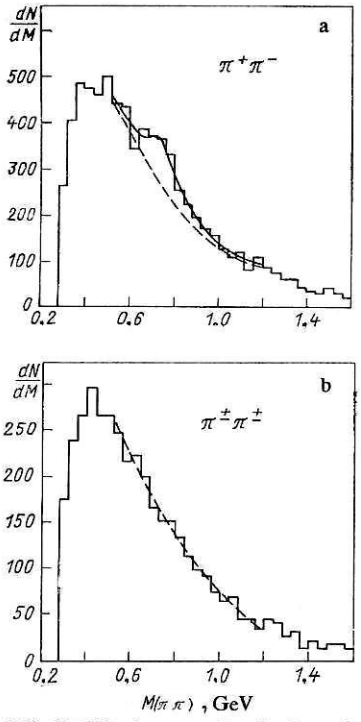

FIG. 15. Effective-mass distributions of pion pairs produced in $\bar{\nu}p$ interactions at $\langle E_{\bar{\nu}}\rangle = 31$ GeV. The broken curve represents the background processes, and the continuous curve takes into account the resonances.

was found that $\langle n(\rho^0)\rangle = 0.14 \pm 0.02$ and $R(\rho^0/\pi^-) = 0.12 \pm 0.02$. The available data on $\langle n(R_i)\rangle$ for ρ^0 and f^0 mesons produced in $\nu(\bar{\nu})N$ interactions are given in Table VII. For comparison we give the values of $\langle n(R_i)\rangle$ for π^+p interactions obtained at approximately the same value of $\langle W\rangle$ ($p = 16$ GeV/c). It can be seen that the fraction of pions produced in $\rho \to \pi\pi$ decays is about 12–15%, as in soft hadron collisions (see Tables I and II). The values of $\langle n(\rho^0)\rangle$ to within the errors (about 25–30%) do not depend on Q^2 for $Q^2 \gtrsim 4\,(\text{GeV}/c)^2$ and increase with increasing W^2 from 10 to 100 GeV^2:

$$\langle n(\rho^0)\rangle = -0{,}08 \pm 0.12 + (0.085 \pm 0.045)\ln(W). \qquad (47)$$

A similar dependence is observed for πp and pp interactions.[56]

The distribution of the ρ^0 mesons with respect to $x_F = p_\parallel^*/p_{\parallel\max}^*$ in the hadron c.m.s. agrees with the x_F distribution of the resonances in the $\pi^+p \to \rho^0 X$ processes at $p = 16$ GeV/c.[56] An appreciable fraction ($\gtrsim 50\%$) of the ρ^0 mesons is produced in the fragmentation region of the u quarks (see Table VI). Figure 16a shows the distributions of the resonances with respect to $x(\rho^0)$ for νp and μN interactions.[56,57] The fraction of pions produced in the decays $\rho^0 \to \pi^+\pi^-$ increases with increasing x (Fig. 16b), and for $x \geqslant 0.6$ we have $R\left(\frac{\rho \to \pi^-}{\pi^-}\right) \approx 1$, i.e., the fragmentation π^- mesons are largely decay products of ρ^0 mesons ($u \to \rho^0 \to \pi^-$). The number of π^+ mesons in this region of x is approximately two times larger than $n(\pi^-)$, and therefore only about 50% of them are produced in the processes $u \to \rho^0 \to \pi^+$. For $\bar{\nu}p$ interactions, in which a d quark frag-

TABLE VII. Production of ρ^0 and f^0 mesons in $\nu(\bar{\nu})p$ and π^+p interactions.

Experiment	$\langle n(\rho^0)\rangle$	$\langle n(f)\rangle$	$\frac{\langle\rho^0\rangle}{\langle\pi^-\rangle}$	$\frac{\langle f\rangle}{\langle\rho^0\rangle}$
νp ($\langle W\rangle = 4{,}4$ GeV)	0.14 ± 0.02	0.04 ± 0.02	0.13 ± 0.02	0.26 ± 0.13
νp ($\langle W\rangle = 4{,}4$ GeV)	$0{,}21\pm0.03$ *	—	—	—
νp ($\langle W\rangle = 5$ GeV)	$0{,}21\pm0.04$	—	—	—
νd ($\langle W\rangle = 5$ GeV)	0.19 ± 0.04	—	0.15 ± 0.04	—
$\bar{\nu}p$ ($\langle W\rangle = 3{,}4$ GeV)	0.21 ± 0.03	—	0.12 ± 0.02	—
π^+p ($p = 16$ GeV/c, $\langle W\rangle = 5{,}56$ GeV)	0.24 ± 0.02	0.050 ± 0.005	0.19 ± 0.02	0.21 ± 0.03

*$\langle n(\rho^0)\rangle$ for events with $n(\pi)\geqslant 1$.

ments, $R(\rho^0/\pi^-) = 0.7 \pm 0.4$ for $x(\rho^0) = 0.6$–0.8 (Fig. 16b).

Thus, at large x the fragmentation $u(d) \to \rho^0$ clearly predominates over $u(d) \to \pi^-$, whereas in some theoretical models it is assumed that they are the same.[2] The distribution of the ρ^0 mesons with respect to $p_\perp^2$ relative to $(\mathbf{p}_\nu - \mathbf{p}_\mu)$ can be described by an exponential with $b = 3.8 \pm 1.0$ $(\text{GeV}/c)^{-2}$, as in soft hadron collisions $[\langle p_\perp(\rho^0)\rangle = 0.46 \pm 0.05$ GeV/c].

In νp interactions, the production of baryon resonances (Δ^{++}, Δ^0) has also been studied.[58] To study Δ^{++} production, 2437 events with total longitudinal momentum of the detected secondary particles satisfying $\Sigma p_\parallel \geqslant 10$ GeV/c were selected.[58] In 455 events, protons with $p \lesssim 1$ GeV/c were identified by means of ionization. In the $M(\pi^+p)$ distribution there is a distinct peak in the region of the Δ^{++} resonance. From this it was found that $R(\Delta^{++}/N_{\text{ev}}) = 0.090 \pm 0.015$ and $R(\Delta^0/N_{\text{ev}}) = 0.013 \pm 0.011$, i.e., about 50% of the protons are produced in $\Delta^{++} \to p\pi^+$ decays. About 75% of the isobars have $x \leqslant 0.2$, i.e., they are produced in the diquark (uu) fragmentation region (see Table VI).

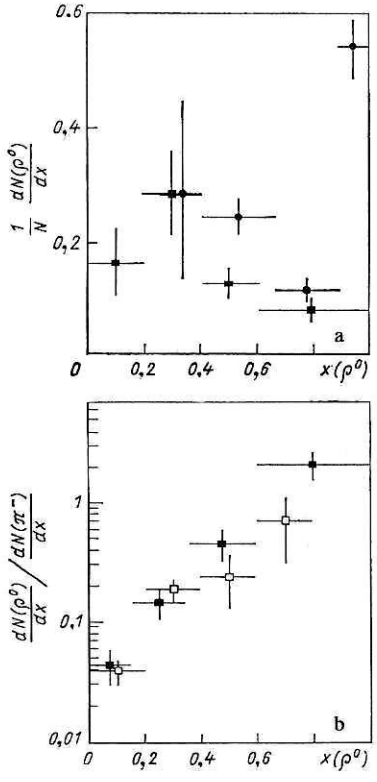

FIG. 16. Distributions of ρ^0 mesons with respect to x in νp and μN interactions (a) and dependence of the ratio $N(\rho^0 \to \pi^-)/N(\pi^-)$ on x for νp and $\bar{\nu}p$ and $\bar{\nu}p$ interactions (b). The black squares, open squares, and black circles correspond to the νp, $\bar{\nu}p$, and μN interactions, respectively.

The production of neutral strange particles (V^0) in lepton–nucleon interactions at high energies has been studied in some experiments.[59–63] In this case, the main role is played by the "elementary" processes

$$\nu d \to \mu^- u + (s\bar{s}), \tag{48}$$

$$\bar{\nu} u \to \mu^+ d + (s\bar{s}), \tag{49}$$

$$e(\mu)\, u \to e(\mu)\, u + (s\bar{s}), \tag{50}$$

in which the strange particles are produced by the "coalescence" of valence quarks (u, d) and sea quarks $(s, \bar{s})$. In addition, according to the data of Ref. 59, about 35% of the neutral strange particles may be produced by decays of charmed particles. Thus, study of the production of V^0 particles makes it possible to obtain direct information about the distributions of the strange and charmed quarks (s, c) in nucleons ($V^0 = \Lambda^0, K^0, \bar{K}^0, \bar{\Lambda}^0$).

In νp interactions ($\langle E_\nu\rangle = 43$ GeV, $\langle W\rangle = 4.6$ GeV), it was found that the fraction of events with neutral strange particles is $17.4 \pm 0.8\%$ and $\sigma(\Lambda)/\sigma(K^0) = 0.26 \pm 0.03$.[59] The distributions of the V^0 particles with respect to the hadron variables (x_F, $p_\perp^2$, and x) are the same for νp, μp, and ep collisions (fragmentation of u quarks; see Table VI) and agree with the anlogous data for π^+p interactions at $p = 16$ GeV/c.[59,62,63] For example, the distributions of the V^0 particles with respect to $p_\perp^2$ in νp collisions can be described by $\exp(-bp_\perp^2)$ with $b(K^0) = 5.3 \pm 0.5$ and $b(\Lambda^0) = 3.5 \pm 0.6$ $(\text{GeV}/c)^{-2}$ ($b_{\pi^+p}(K^0) = 5.60 \pm 0.08$ and $b_{\pi^+p}(\Lambda^0) = 3.48 \pm 0.09$). In Ref. 61, the polarization of the Λ^0 particles in $\bar{\nu}p$ interactions was also estimated: $P(\Lambda^0) = 0.34 \pm 0.18$.

Th agreement of the distributions $x(K^0)$ for weak and electromagnetic interactions when $x \gtrsim 0.4$ (fragmentation region of the u quarks) makes it possible to obtain the first information about the fragmentation function $D_u^{K^0}(x)$. Unfortunately, the statistics of the events with K^0 mesons is still poor (359 K_S^0).[59]

In the distributions with respect to the effective masses

$M(K^0\pi^+)$ and $M(\Lambda\pi^+)$ signals have been found ($r \lesssim 0.5$–0.3) of the resonances $K^{*+}(890)$ and $\Sigma^+(1385)$.[59] It was estimated that they are produced in $5.5 \pm 2.0\%$ and $1.4 \pm 0.4\%$ of the total number of $\nu p \to \mu^- X$ events, respectively, for $W'(K^*) \geqslant 1.8$ and $W'(\Sigma^+(1385)) \geqslant 1.5$ GeV [$W'(R_i)$ are the production thresholds of the resonances]. Similar results were obtained for νp interactions.[60,61]

Thus, the first data on the production of resonances and hadrons in deep inelastic lepton–nucleon interactions show that the mechanisms of their production are similar to those in strong interactions. Unfortunately, the statistics of the events for lN collisions is still low (2000–8000 events), they have been obtained for a wide range of energies, and the mean total energies of the secondary hadrons are not large ($\langle W \rangle \lesssim 6$ GeV), which is equivalent to hN interactions at $p = 16$–20 GeV/c.

High-Energy e^+e^- Interactions

For the study of $q \to \Sigma h$ transitions, e^+e^- annihilation processes are the most promising[54]:

$$e^+ + e^- \to \gamma^* \to q + \bar{q} \to \Sigma h_i + \Sigma h_j. \tag{51}$$

In this case, the entire primary energy is expended on the production of point quarks, which then fragment into hadrons. Most of the data on the reactions (51) at high energies have been obtained using the accelerators with colliding electron and positron beams at Hamburg in the German Federal Republic and at Stanford in the United States ($\sqrt{s} \leqslant 36$ GeV).

Investigations of e^+e^- interactions at high energies made it possible to test quantum electrodynamics down to distances $(1$–$2) \times 10^{-16}$ cm, to discover new particles ($J/\psi, \tau$, etc.), and to study lepton–quark interactions. To a large degree, QCD and the quark–parton models are based on e^+e^- annihilation data, and we shall therefore briefly list the main results.[1,2,54]

The total cross section $[\sigma_{\text{tot}}(W)]$ of processes of the type (51) has been measured at $W \leqslant 36$ GeV. In QCD, its ratio to $\sigma_{\text{tot}}(e^+e^- \to \mu^+\mu^-)$ is determined by the expression[54]

$$R = \frac{\sigma(e^+e^- \to h)}{\sigma(e^+e^- \to \mu^+\mu^-)} = 3\sum_q e_q^2 \left\{1 + \frac{\alpha_S(Q^2)}{\pi} + O(\alpha_S^2)\right\}, \tag{52}$$

where the factor 3 is due to the three different quark colors; e_q is the electric charge of the quarks; and $\alpha_S(Q^2)$ is their coupling constant at momentum transfers Q^2. In the parton model, $\alpha_S(Q^2) = 0$.[2] In the lowest order of perturbation theory,

$$\alpha_S(Q^2) = \frac{12\pi}{(33 - 2N_q)\ln(Q^2/\Lambda^2)}, \tag{53}$$

where N_q is the number of different quarks (u, d, s, c, b) and $\Lambda \approx 0.2$–0.3 GeV is the parameter that characterizes the region of applicability of QCD ($Q^2 > \Lambda^2$). For $W \gtrsim 20$ GeV about the production threshold of the known quarks

$$3\sum_{u,d,s,c,b} e_q^2 = 11/3$$

and

$$R = 11/3\left\{1 + \frac{\alpha_S(Q^2)}{\pi} + O(\alpha_S^2)\right\}. \tag{52'}$$

The experimental values of $R(W)$ in this range of energies do not depend on W to within the errors,[54] and

$$\langle R_{\text{exp}}(W) \rangle = 4.01 \pm 0.03(\text{stat}) \pm 0.20(\text{syst}),$$

where the statistical and systematic errors are given. Comparing R and R_{exp}, we obtain

$$\alpha_S = 0.18 \pm 0.03(\text{stat}) \pm 0.14(\text{syst}). \tag{54}$$

Here, the systematic errors in the determination of α_S are large, but the color nature of the quarks [the factor 3 in (52)] is established unambiguously.

After production, the $q\bar{q}$ pairs fragment into hadrons which are collimated around the direction of emission of the quarks. The degree of collimation is proportional to W^{-1} and varies from $\delta \approx 31°$ ($W = 4$ GeV) to $\delta \approx 17°$ ($W = 36$ GeV), where δ is half the angle of the emission cone of the hadrons relative to the emission axis of the quarks.[54] Therefore, the identification of hadron jets in e^+e^- annihilation at high energies is simpler and more unambiguous than in hard and deep inelastic processes. The distribution of the jet axis with respect to the angle (θ_J) relative to the direction of the primary particles can be well described by the formula

$$W(\cos\theta_J) \sim (1 + \cos^2\theta_J), \tag{55}$$

which holds for the production of photons by $q\bar{q}$ particle pairs with spin $J = \frac{1}{2}$.

A triumph of QCD was the prediction and detection of hard gluon emission processes[65–67]:

$$e^+ + e^- \to q + \bar{q} \to q' + \bar{q}' + g. \tag{56}$$

In this case, three hadron jets are produced in the final state,

$$e^+ + e^- \to q + \bar{q} + g \to \sum_q h_i + \sum_q h_j + \sum_g h_k, \tag{57}$$

and these were discovered in 1979 at $W = 30$–36 GeV.[66] The three-jet events are about 10% of all $e^+e^- \to h$ annihilations, and their cross section

$$\sigma(e^+e^- \to q\bar{q}g) \sim \sigma(e^+e^- \to h)\,\alpha_S(Q^2) \tag{58}$$

is proportional to $\alpha_S(Q^2)$.

From the data obtained on $\sigma(e^+e^- \to q\bar{q}g)$ it was found that

$$\alpha_S(Q^2) = 0.17 \pm 0.01(\text{stat}) \pm 0.03(\text{syst}). \tag{59}$$

Study of the characteristics of the three-jet events also made it possible to determine the gluon spin [$J(g) = 1$].[54,66,67]

Thus, the basic postulates of QCD and of the quark–parton model[1,2] on the interaction of point particles (quarks and leptons) for $Q^2 > \Lambda^2$ were brilliantly confirmed in experiments on e^+e^- interactions. The main unresolved problem remained the mechanism of the quark transitions into hadrons (the confinement problem). Therefore, this stage of all the particle interaction processes is described by means of phenomenological models with parameters whose values are determined from the experimental data (see Sec. 4).

In e^+e^- annihilation, data have so far been obtained only on the characteristics of the secondary long-lived hadrons ($\pi, K, p, \bar{p}, \Lambda, \bar{\Lambda}$), and these can be to a large degree determined by the decay kinematics of the resonances; this applies especially to the pions and kaons (see Sec. 2). Nevertheless, the observed similarity of their behavior in weak,

strong, and electromagnetic interactions is probably due to the universal nature of quark fragmentation into hadrons and makes it possible to obtain data on the fragmentation function $D_q^h(x, p_\perp^2)$.

Characteristics of Secondary Hadrons in e^+e^-, lN, and hN Interactions

The lepton–quark nature of all particle interactions makes it possible to obtain data on quark fragmentation into hadrons from simultaneous analysis of multiparticle production processes in weak, electromagnetic, and strong interactions. In comparing data, one must bear in mind the differences between the energies and states of the fragmenting systems. In e^+e^- annihilation, the initial state is, as a rule, a $q\bar{q}$ pair (51) with energy $2E_q = W = \sqrt{s}$, all of which is expended on producing the hadrons. In lN interactions, it is a quark and a diquark that fragment, and their total energy W is much less than the energy of the primary particles ($\sqrt{s}$ (Fig. 17a). The situation in hN interactions is more complicated. Here we have the production of four jets of hadrons, a good separation of which is possible only at high energies ($E \gtrsim$ 1–2 TeV).[48] Two hadron jets are associated with the quark interaction (34), and two spectator jets are produced on the fragmentation of the quarks (diquarks) that did not interact (Fig. 17b).

To determine the energy expended on hadron production in each jet, one uses a jet separation method similar to the one developed for e^+e^- interactions, or one simply eliminates from consideration the so-called leading particles ($x \geqslant 0.4$) (to separate the jets from the quarks that did not interact).[7,68] For example, for pp interactions protons with $x \geqslant 0.4$ are eliminated. In this case, it can be assumed that the energy that is passed to the hadrons produced on the quark fragmentation (34) is $W = \sqrt{s} - E_p^{(1)} - E_p^{(2)}$. Therefore, data obtained in different processes are compared at the same W but not the same $\sqrt{s}$ for the primary particles.

Another important question in comparing the data is the species of the quarks that fragment into hadrons (see Table VI). It is different for different processes, and, as a rule, diquarks fragment in the target fragmentation region. Therefore, when comparing data it is desirable to select processes in which the same quarks (diquarks) fragment. Unfortunately, this is in practice impossible at the present accuracy of experiments.

We begin our consideration of the data with the multiplicity of the charged secondary particles in hN, e^+e^-, and lN interactions. At relatively low energies ($W \lesssim 10$ GeV), the mean multiplicity of the charged particles [$\langle n_{ch}(W)\rangle$] increases slowly with increasing W ($\sim \ln W$) and to within the errors does not depend on the type of interaction (Fig. 18).[5,7] At higher energies, there are data on $\langle n_{ch}(W)\rangle$ in e^+e^- annihilation and in pp interctions.[68] The absolute values of $\langle n_{ch}(W)\rangle$ obtained in e^+e^- interactions by means of different facilities differ by 5–10%. This is due to the methodological difficulties of detecting all particles and eliminating background processes (of the type $e^+e^- \to K_S^0 \to \pi^+\pi^-$). To within the errors, there are no differences between the data for pp and e^+e^- interactions (Fig. 18). At $W \gtrsim 7$ GeV, a rapid growth of $\langle n_{ch}(W)\rangle$ is observed; it can be satisfactorily described by the expression

$$\langle n_{ch}(W)\rangle = n_0 + a \exp\left(b\sqrt{\ln(W^2/\Lambda^2)}\right), \qquad (60)$$

which is obtained in the framework of QCD.[69] Here, $\Lambda = 0.3$ GeV, $n_0 = 2.5 \pm 0.1$, $a = 0.030 \pm 0.004$, and $b = 1.9 \pm 0.1$. What is the cause of this growth of $n_{ch}(W)$? Estimates show that it cannot be explained by an increase in the cross section of the hard gluon bremsstrahlung (57).[54] Through these processes one expects a growth of $\langle n_{ch}(W)\rangle$ by 0.8 at $W = 35$ GeV ($\Delta n_{ch} \approx 0$ at $W \lesssim 10$ GeV). It is possible that the growth in $\langle n_{ch}\rangle$ is mainly due to the increase in the phase space ($\sim W^{1/2}$).[54] It is interesting to note that the new data[70] on $\bar{p}p$

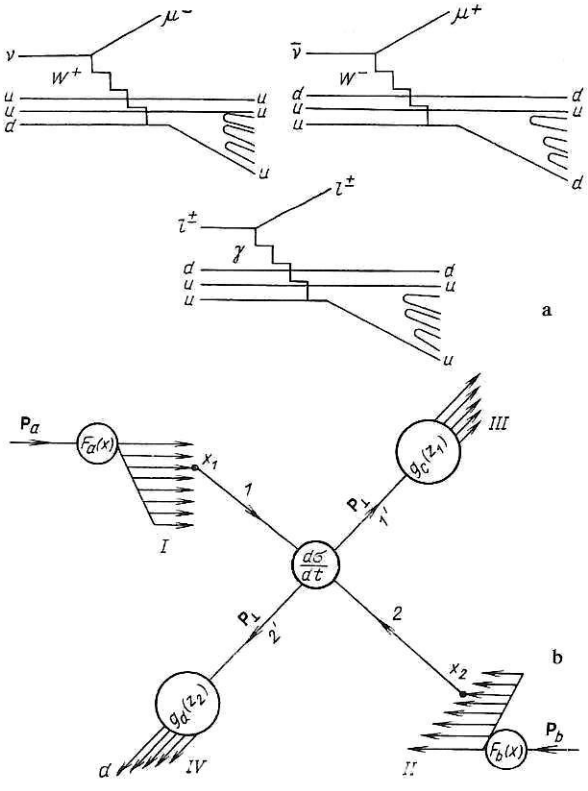

FIG. 17. Diagrams of lepton interaction with quarks (a) and scheme of hard hadron collisions (b).

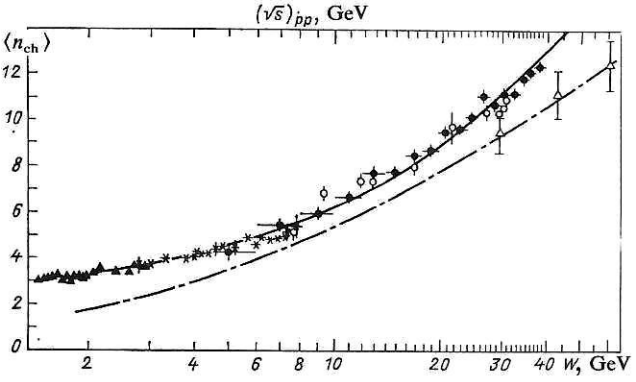

FIG. 18. Dependence of $\langle n_{ch}\rangle$ on the total energy W of the secondary hadrons. The black circles and open triangles correspond to pp interactions, the black triangles, asterisks, and open circles to e^+e^- annihilation; the continuous curve is calculated in accordance with Eq. (60), and the chain curve gives the dependence of $\langle n_{ch}\rangle$ on $\sqrt{s}$ for pp collisions.

interactions at $\sqrt{s} = 540$ GeV can be satisfactorily described by the dependence

$$\langle n_{ch}(s)\rangle = a_1 + b_1 \ln s + c_1 \ln^2 s, \quad (61)$$

which is obtained when $\langle n_{ch}(s)\rangle$ is analyzed in pp collisions for $\sqrt{s} \leqslant 63$ GeV.[5,7] In this case, there is no rapid growth of $\langle n_{ch}(s)\rangle$ with the energy, as there was for $\sqrt{s} \leqslant 63$ GeV without elimination of the leading particles.[68] Interest therefore attaches to obtaining data on $\langle n_{ch}(W)\rangle$ for events without leading particles at $\sqrt{s} = 540$ GeV.

The actual multiplicity distribution $P(n_{ch}(W))$ for e^+e^- annihilation satisfies KNO scaling[5,7]:

$$\langle n_{ch}\rangle P(n_{ch}) = \psi\left(\frac{n_{ch}}{\langle n_{ch}\rangle}\right), \quad (62)$$

i.e., does not depend explicitly on the energy ($W = 10$–36 GeV). However, the distribution (62) is narrower than the corresponding $\psi(pp)$ without elimination of the leading particles.

The composition of the secondary particles in e^+e^- annihilation (Fig. 19) varies with increasing momentum of the secondary particles in the same way as occurs in hN interactions (see Sec. 3).[54,71] For example, at $W = 30$ GeV and $p \approx 0.3$ GeV/c about 90% of the secondary particles are $\pi^\pm$ mesons, while $\lesssim 10\%$ are $K^\pm$ mesons. With increasing momentum, the fraction of heavy particles ($K, p, \bar{p}$) increases; at $p = 4$–6 GeV/c, about 55% are $\pi^\pm$ mesons, $\approx 33\%$ are $K^\pm$ mesons, and 12% are p and $\bar{p}$. At even higher momenta ($p \approx 10$ GeV/c), the $\pi^\pm : (K^0, \bar{K}^0) : (\Lambda^0, \bar{\Lambda}^0)$ ratios are 4:2:1. A large proportion of kaons and baryons is also found in hard hadron collisions at $p_\perp \gtrsim 3$ GeV/c (see Sec. 3). For comparison, Table VIII gives estimates of $\langle n_i\rangle$ for e^+e^- annihilation ($W = 30$ GeV) and soft pp interactions ($\sqrt{s} = 52.5$ GeV).[53,54] The errors in the determination of $\langle n_i\rangle$ are 10–15%. It can be seen from this that in deep inelastic processes ($e^+e^- \to h$) more heavy particles ($K, p, \bar{p}, \Lambda$) are produced than is the case in soft hadron collisions.

The distributions of the long-lived hadrons with respect to the momenta (transverse and longitudinal with respect to the axis of the hadron jet) are to a large degree similar for different types of interactions (e^+e^-, lN, hN).

The mean longitudinal momentum $\langle p_\parallel\rangle$ of the hadrons increases in proportion to W and varies from 0.4 ($W \approx 5$ GeV) to 1.3 GeV/c ($W = 30$ GeV).[54,72] The mean transverse momentum $\langle p_\perp\rangle$ increases with increasing W from 0.34 to 0.45 GeV/c in the same range of W. From this it is possible to estimate the half-angle of the emission cone of the particles in the jet: $\delta \sim \langle p_\perp\rangle / \langle p_\parallel\rangle \sim 20°$ at $W = 30$ GeV (see Sec. 3). With increasing energy, the distribution $\frac{1}{\sigma}\frac{d\sigma}{dp_\perp^2}$ itself becomes broader. This effect is well described in QCD and is due to the hard bremsstrahlung (56) of gluons, whose mean transverse momentum satisfies $\langle k_\perp(g)\rangle \sim \alpha_s W$.[54,66] It is the appearance of a third (gluon) jet of hadrons that leads to the growth of $\langle p_\perp\rangle$ and $\langle p_\perp^2\rangle$ with increasing W ($\gtrsim 10$ GeV) when the events are analyzed in accordance with a two-jet model ($e^+e^- \to q\bar{q}$). Analysis of the data at $W = 30$ GeV with allowance for the production of three jets ($e^+e^- \to q\bar{q}g$) showed that the distributions of the hadrons with respect to $p_\perp^2$ relative to the axis of "their' jet do not differ from $\frac{1}{\sigma}\frac{d\sigma}{dp_\perp^2}$ at $W = 12$ GeV, when gluon emission can be ignored and $\langle p_\perp\rangle = 0.3$–$0.35$ GeV/c.[66,71] Thus, in a first approximation it can be assumed that the distributions of the hadrons with respect to x and $p_\perp^2$ do not depend on W and are the same for quarks and gluons.

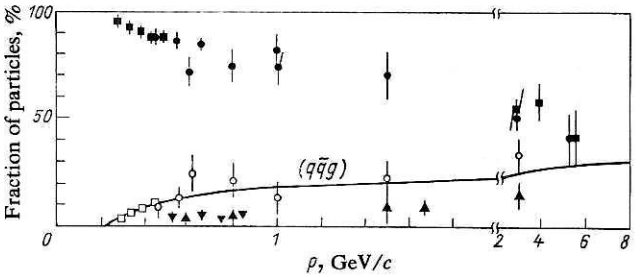

FIG. 19. Fraction of particles of a given species (%) in the total number of secondary charged particles as a function of the momentum at $W = 30$ GeV (e^+e^- annihilation). The curve shows the contribution of hard gluon emission to the production of $K^\pm$ mesons ($q\bar{q}g$): $\pi^\pm$ (black squares and black circles), $K^\pm$ (open squares and open circles), and $p + \bar{p}$ (black inverted triangles and black triangles).

As we have already noted (see Secs. 1 and 2), the data on lepton–nucleon interactions were obtained mainly at $W \lesssim 10$ GeV, and therefore a violation of $p_\perp^2$ scaling for hadrons was not found.[53] In hard hadron collisions, hadron jets at $W = 2$–14 GeV have also been studied, and it has been found that $\langle p_\perp\rangle \approx 0.4$–$0.5$ GeV/c with no dependence of W.[48] First data have also been obtained on the characteristics of hadron jets in soft hadron collisions for πp, Kp, and pp interactions ($\sqrt{s} = 9$–62 GeV).[72–75] Although the actual existence of jets similar to the jets from quarks is problematic in soft hadron interactions, the characteristics of the hadrons in them and in the processes (51) were found to be remarkably similar. We have already noted the same dependence (60) of $\langle n_{ch}\rangle$ on W. Also the same are the distributions of the hadrons with respect to $p_\perp / \langle p\rangle$ for $W = 8$–30 GeV ("scaling on the average").[73] There are differences between $\frac{1}{\sigma}\frac{d\sigma}{dp_\perp^2}$ at $W = 28$–32 GeV. In pp interactions, these distributions are somewhat narrower than in e^+e^- annihilation. This may be due to the

TABLE VIII. Mean multiplicities of particles in e^+e^- annihilation ($W = 30$ GeV) and in pp interactions ($\sqrt{s} = 52.5$ GeV).

Type of reaction	π^+	π^0	$K^\pm$	p	$\bar{p}$	Λ^0	$\bar{\Lambda}^0$	$\langle n_{ch}\rangle$
$e^+e^- \to h_i X$	11	5.5	1.4	0.2	0.2	0.15	0.15	12.8
$pp \to h_i X$	9	4.7	0.73	1.62	0.14	0.13	0.08	11.5

crude method of eliminating the spectator jets. At lower energies ($W \lesssim 20$ GeV), these distributions do not differ.

The distributions of the hadrons in a jet with respect to the total (or longitudinal) momenta, measured in fractions of the jet energy ($x = 2p/W$), hardly depend on W when $W \gtrsim 510$ GeV and $x \gtrsim 0.15$ (Fig. 20).[54,71] At large W, when the particle masses can be ignored, the cross sections of e^+e^- annihilation can be represented in the form

$$\frac{d\sigma}{dx}(e^+e^- \to q\bar{q} \to h) = \sigma_{\text{tot}}(q\bar{q})\, 2D_q^h(x, s) = \frac{8\pi\alpha^2}{s} e_q^2 D_q^h(x, s), \quad (63)$$

where $D_q^h(x, s)$ is the number of hadrons with energy x and $\sigma(q\bar{q})$ is the cross section for the production of $q\bar{q}$ pairs. In this case, it follows from the scaling $f(x) = sd\sigma/dx$ that the fragmentation function $D_q^h(x)$ is independent of the energy (Fig. 20). At small x ($\lesssim 0.15$), the particle yield increases sharply as W increases from 5 to 35 GeV. It is this that explains the rapid growth (60) of the mean multiplicity of the charged particles in e^+e^- annihilation. It occurs because of the increase in the multiplicity of the low-energy particles ($p \lesssim 1$ GeV/c). There is a similar effect in pp interactions.[5,7] The function $D_q^h(x)$ also changes slightly when $x \gtrsim 0.4$. Its values decrease with increasing energy. A departure from scaling of this type is expected in QCD because of the increase in the cross section $\sigma(e^+e^- \to q\bar{q}g)$, which naturally leads to a decrease in the yield of hadrons

The distributions of the hadrons with respect to the rapidity ($y = \frac{1}{2}\ln\frac{E + P_\parallel}{E - P_\parallel}$ relative to the jet axis reveal the existence of a plateau whose height increases with increasing W by about three times in the interval 5–32 GeV.[71] The width of the plateau also increases, and at $W = 32$ GeV it is about three units.

These same features in the behavior of $D_q^h(x)$ are characteristic for the individual species of particles ($\pi^\pm$, $K^\pm$, $K^0, \bar{K}^0, p, \bar{p}, \Lambda, \bar{\Lambda}$), produced in e^+e^- annihilation (Figs. 21 and 22). For $x \gtrsim 0.1$, $D_q^h(x) \sim \exp(-8x)$ and this function is the same for different particles. The large yield of kaons at $x \geqslant 0.3$ is remarkable, since only about 30% of them are produced by valence quarks (s, c, b)—the remainder are produced by sea quarks.[2,54] The most unexpected result is the large yield of baryons. Exotic models are invoked to describe it.[54] For example, it is assumed that there is a significant probability of removal from the vacuum of not only a $q\bar{q}$ pair but also a $qq\bar{q}\bar{q}$ state [$P(qq)/P(q) \approx 0.08$]. A different explanation of the large baryon yield can be given in the framework of the additive quark model (see Sec. 4).

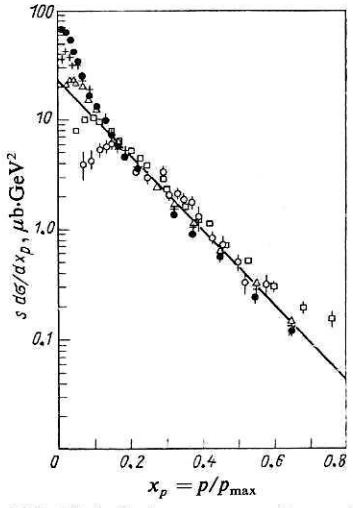

FIG. 20. Inclusive spectrum of secondary charged particles produced in e^+e annihilation at $W = 5$–34 GeV: the open circles, open squares, open triangles, plus signs, and black circles correspond to 5, 7.4, 14, 22, and 34 GeV, respectively.

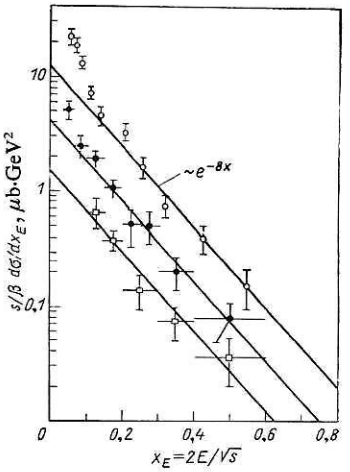

FIG. 21. Distributions of $\pi^\pm$ (open circels), K^0 ($\bar{K}^0$) (black circles), and Λ ($\bar{\Lambda}$) (open squares) produced in e^+e^- annihilation ($W = 33$ GeV) with respect to $x_E = 2E/\sqrt{s}$.

In hard hadron collisions, the fragmentation function $D_q^h(x)$ is also independent of the energy for $W = 5$–16 GeV and $x \gtrsim 0.3$[48,74] At smaller values, $D_q^h(x)$ behaves in the same way as in e^+e^- annihilation. In soft pp collisions, the distributions of the hadrons with respect to x (after elimination of the leading protons) agree well with the analogous hadron distributions in e^+e^- annihilation at $W = 3$–30 GeV.[74]

In deep inelastic lepton–hadron interactions [ep, μp, $\nu(\bar{\nu})p$] the distributions of the hadrons with respect to x were analyzed in the fragmentation regions of the "knocked-out" quark ($x_F \geqslant 0$) and the remaining diquark ($x_F < 0$), although the energies ($W \leqslant 10$ GeV) were still small for separating these regions.[53,55] As a rule, these distributions were compared with data on $D_q^h(x)$ obtained in pp and e^+e^- interactions at equal energies (see, for example, Fig. 23). As can be seen from Fig. 23, the values of $D_q^h(x)$ do not differ from each other to within the errors for $x \gtrsim 0.1$ in the fragmentation region of the "knocked-out" quark, although the types are different (see Table VI). The statistical errors and systematic uncertainties in the various experiments are too large, and the energies too low for confident separation of fragmentation of the different quarks (u, d, s). Nevertheless, such attempts have been made.[53,55] For example, the x_F distributions of the $h^\pm$ hadrons in $\bar{\nu}p$ interactions were analyzed in accordance with the expression

$$f(x_F) = A(1 - |x_F|)^n$$

in the fragmentation regions of the target ($ud \to h^\pm$) at

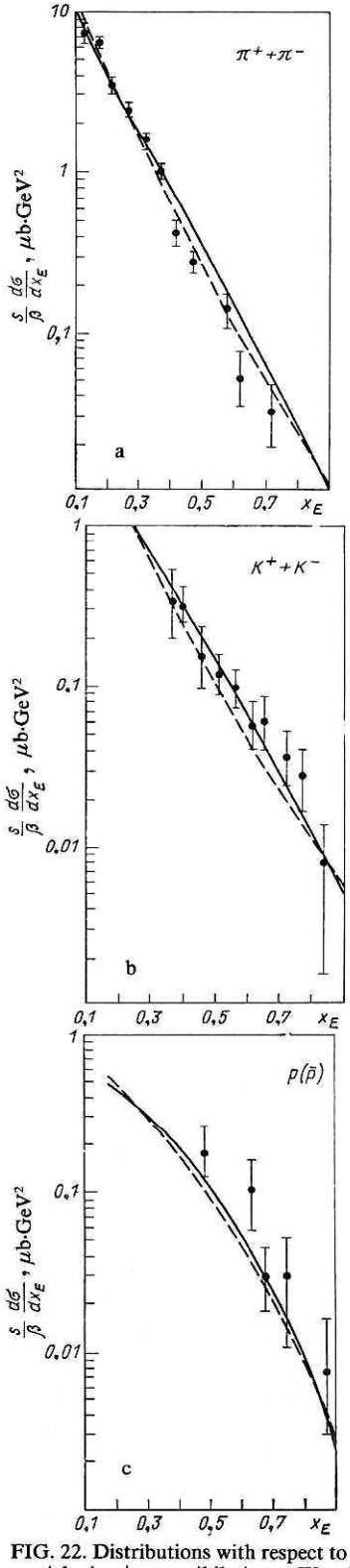

FIG. 22. Distributions with respect to x_E of $\pi^\pm$ (a), $K^\pm$ (b), and p ($\bar{p}$) (c) particles in e^+e^- annihilation at $W = 4$–5 GeV. The curves are the results of calculations in accordance with the additive quark model (see Sec. 4).

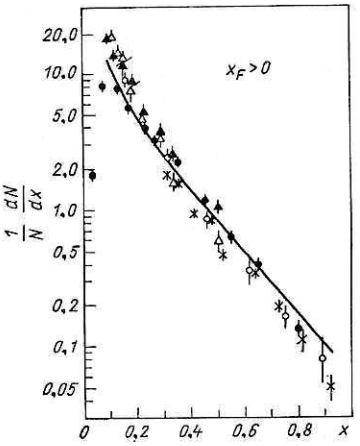

FIG. 23. Distributions with respect to x of secondary charged hadrons produced in deep inelastic processes, in e^+e^- annihilation, and in pp collisions: black circles $\bar{\nu}N$; open circles and crosses, ep; open triangles, $\frac{1}{2}(e^+e^- \to h)$; black triangles, $\frac{1}{2}pp$.

$x_F \leqslant -0.05$ and the knocked-out" quark d ($x_F \geqslant 0.05$).[55] The values obtained for n (Table IX) agree to within the errors with n_{exp} for K^+p interactions at $p = 32$ GeV/c (see Table IV), although the fragmenting systems of quarks are different (see Table VI). When the energy W is increased, especially for deep inelastic interactions, it will be possible to measure $D_q^h(x)$ for different quark species.

Thus, at the present time it can be assumed that in a first approximation the fragmentation functions $D_q^h(x, p_\perp^2)$ of the quarks are approximately the same in different types of interactions. For $W \gtrsim 5$ GeV and $x \gtrsim 0.2$ they do not depend on the energy, and $D(x) \sim \exp(-8x)$ for pions, kaons, and baryons. The first data on gluon fragmentation into hadrons ($e^+e^- \to q\bar{q}g \to h$) show that there is no large difference between $D_q^h(x, p_\perp^2)$ and $D_g^h(x, p_\perp^2)$. The mean transverse momentum of the long-lived hadrons in a jet is $\langle p_\perp \rangle \approx 0.3$–$0.35$ GeV/c in a wide range of energies ($W = 5$–36 GeV). However, the first results in the investigation of the production of resonances in deep inelastic particle collisions show that their fraction is large (greater than 5–60%), as in soft hadron interactions. Therefore, $\langle p_\perp \rangle$ of the directly produced particles in the jet is larger and according to the estimates is about 0.5 GeV/c. In this connection, the question of the nature of the x distributions of the hadrons and resonances arises. They may differ, especially for pions and kaons (see Sec. 2). Then the form of the true fragmentation function $D_q^R(x, p_\perp^2)$ will be different from the measured function. However, its scaling properties will hardly change.

4. QUARK–PARTON PICTURE OF MULTIPARTICLE PRODUCTION AND HADRON STRUCTURE

The modern picture of multiparticle production processes is based on the interactions of point particles—leptons

TABLE IX. Values of n for $\bar{\nu}p$ interactions [$f(x_F) = (1 - |x_F|)^n$].

x_F	Particle species	n
$\leqslant -0.05$	h^+	3.0 ± 0.3
$\leqslant -0.05$	h^-	3.3 ± 0.5
$\geqslant 0.05$	h^+	2.0 ± 0.2
$\geqslant 0.05$	h^-	1.6 ± 0.2

and quarks.[1,2] It is particularly clearly revealed in the first stage of these processes at high momentum transfers, when the quarks can be regarded as being free [$\alpha_s(Q^2) \to 0$] (see Sec. 3). In this case, the quark-parton model with free quarks is a good approximation, and the deviations from it can be described by QCD.[2] However, for the last stage of these processes (the transition of the quarks into hadrons) QCD is not valid because of the growth of $\alpha_s(Q^2)$ (the confinement problem), and it is described by means of phenomenological models with several free parameters, whose values are determined from the experimental data (Refs. 2, 5, 7–12, 18, and 32–36). These parameters can be used to establish the main features of hadron structure and quark-fragmentation processes.

We shall discuss the theoretical interpretation of only the general features of these processes that can be regarded as established. These include:

1. The universal nature of the distributions of the resonances with respect to the transverse and longitudinal momenta (see Sec. 2).

2. The copious production of resonances and the small fraction of pions and kaons among the secondary particles produced in particle interactions at high energies (see Secs. 2 and 3).

3. The universality of the characteristics of the hadron jets in deep inelastic collisions, hard particle collisions, and e^+e^- annihilation (see Sec. 3). The fraction of heavy particles, especially baryons, in hadron jets is large.

4. The similarity of the characteristics of the hadrons in all types of particle interaction (see Sec. 3).

To describe multiparticle production processes, a wide spectrum of models is used, these ranging from classical to quantum-chromodynamic models (Refs. 2–12, 18, and 32–36). Even a brief discussion of them would require a special review. However, if we consider only the features listed above and the models based on the quark–parton picture of particle interaction, we can restrict ourselves to two popular models: the fragmentation model for deep inelastic and hard particle collisions[2] and the additive quark model,[18,32–36] which describe multiparticle processes and complement each other.

In the original version of the additive quark model,[18] only the symmetry properties of quark interactions in soft particle collisions were considered. The model contained two basic assumptions, which are also used in modern modifications of the model.[32–36]

The first relates to the concept of constituent or "dressed" quarks (in Ref. 38, they are called valons).[18,32] In contrast to current (point) quarks, a constituent quark is a complicated system formed by a valence quark and the sea of quark–antiquark pairs and gluons. The effective masses of the constituent quarks are deduced either from the hadron masses or from the magnetic moments of the baryons.[32] In all cases, the results are similar: $M(u) \approx M(d) \approx 350$ MeV and $M(s) - M(u) \approx 175$ MeV.

In the additive quark model, the properties of the hadrons and their soft interactions are determined by the characteristics of the constituent quarks, which are assumed to be almost independent (impulse approxiations). The constituent quarks carry the fraction $x = 1/3$ of the baryon modmentum and 1/2 of the meson momentum. As a rule, the interaction of hadrons reduces to the interaction of two quarks, which results in the production of new quarks in the central region ($|x| \lesssim 1/6$) and in the fragmentation regions ($|x| \gtrsim 1/3$) of the spectator quarks (Fig. 24; see Refs. 5, 18, and 32–36).

The combination of these quarks leads to the production of the hadrons. The rules of this transition form the second basic assumption of the additive quark model.[18] They are as follows. At high energies, many quarks and antiquarks are produced in the central region. The quark model is $SU(6)$-symmetric, and it is therefore natural to assume that the probability of quark and antiquark production depends neither on their species and quantum numbers (flavor, color, spin, etc.) nor on the original colliding quarks. In this case, the probability of finding a quark or antiquark with arbitrary rapidity is the same ($\frac{1}{2}q + \frac{1}{2}\bar{q}$). The probability that there will be a quark or antiquark close to it in rapidity is also the same:

$$\left(\tfrac{1}{2}q+\tfrac{1}{2}\bar{q}\right)\left(\tfrac{1}{2}q+\tfrac{1}{2}\bar{q}\right) \to \tfrac{1}{4}qq+\tfrac{1}{4}\bar{q}\bar{q}+\tfrac{1}{2}q\bar{q} \to \tfrac{1}{4}qq+\tfrac{1}{4}\bar{q}\bar{q}+\tfrac{1}{2}M, \tag{64}$$

where M is a $q\bar{q}$ meson state. Continuing this combination,[3,4,35] we obtain for the central $(q, \bar{q})_s$ region[8)]

$$(q, \bar{q})_s \to N(s)\ (6M + B + \bar{B}), \tag{65}$$

where $B = qqq$ and $\bar{B} = \bar{q}\bar{q}\bar{q}$ are the baryon states of the quarks, and $N(s)$ depends on the total energy ($\sqrt{s}$) of the colliding quarks and determines the growth of the mean multiplicity of the hadrons with the energy, for example, $N(s) = b \ln(s/s_0)$. The parameters b and s_0 are the same for all processes and are taken from an analysis of experimental data.[34,35]

The additive quark model predicts[18] that the ratios of the yields of mesons and baryons are

$$M : B : \bar{B} = 6 : 1 : 1, \tag{66}$$

and an equal probability for the production of the components of $SU(6)$ multiplets. Similarly, one can obtain the relations between B and M yields in the fragmentation regions[34,35]:

$$q_i \to \frac{1}{3}B_i + \frac{2}{3}M_i, \tag{67}$$

$$(q_iq_j) \to \frac{1}{2}B_{ij} + \frac{1}{12}(B_i + B_j) + \frac{5}{12}(M_i + M_j), \tag{68}$$

where q_i and q_iq_j are the fragmenting spectator quarks. The

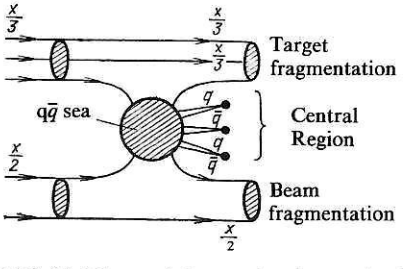

FIG. 24. Scheme of pion–nucleon interaction in the additive quark model.

[8)]The subscript s means that sea quarks participate in the combination.

baryon and meson states with indices i and j contain the initial fragmenting quarks $M_i = q_i\bar{q}$, $M_j = q_j\bar{q}$, $B_i = q_iqq$, $B_{ij} = q_iq_jq$). The ratio of mesons to baryons for the fragmentation (67) of one quark q_i is

$$M : B = 2 : 1 \tag{69}$$

and for fragmentation of two quarks (q_iq_j) it is

$$M : B = 5 : 4. \tag{70}$$

The fraction of baryons in the fragmentation region is larger than in the central region.

Ther relations (65)–(70) are valid as $s \to \infty$. At finite energies ($E \lesssim 2$ GeV), it is well known that strange particles, which contain the strange quark (s), are produced much less often than nonstrange particles (see Sec. 2). It is possible that this is due to the strange quark being relatively heavier, which has an effect at finite energies. In this connection, one introduces a parameter λ characterizing[34,35] the suppression of the production of strange quarks ($\lambda = 0.3$ at $E \lesssim 2$ TeV).

The meson and baryon states of the constituent quarks for real hadrons. Analysis of the experimental data shows that mainly baryons and mesons from the first $SU(6)$ multiplets are produced, namely, baryons from the 56-plet and mesons from the 36-plet with zero orbital angular momentum of the quarks ($L = 0$). This means that the baryon states (qqq) are represented by the octet of particles with $J^P = 1/2^+$ and decuplet with $J^P = 3/2^+$, and the mesons ($q\bar{q}$) by the two nonets with $J^P = 0^-$ and $J^P = 1^-$. In addition, it has been shown that the meson multiplets with $L = 1$ (P–wave meson states) constitute not less than 25% of all the mesons produced directly in multiparticle reactions.[33] The contribution of multiplets with $L = 2$ is estimated at about 10%.[34,35] Baryon states with $L = 1$ and 2 are also probably produced, but as yet it is difficult to estimate their contribution. In Refs. 18 and 33–35 there are tables of the relative probabilities of hadron production with allowance for the suppression of the production of strange quarks (λ) and multiplets with $L = 1$ and 2.

We summarize the basic predictions of the additive quark model based on the introduction of constituent quarks and quark combinatorics (or quark statistics). In soft particle collisions, the hadrons are produced in the central region ($|x| \lesssim 1/6$) and in the fragmentation region of the constituent spectator quarks ($|x| \gtrsim 1/3$) (see Fig. 23). In the central region, many of them are produced in accordance with (65) and (66), and the yields of the different hadrons depend neither on their quantum numbers nor on the species of the primary particles. In this connection, the model predicts the same universal distribution of the directly produced particles with respect to the longitudinal and transverse momenta (item 1 in the list of general features of resonance production; see Sec. 2). In the fragmentation regions, these distributions depend only on the x of the quarks fragmenting in accordance with (67) and (68), as is observed in experiments for pp, πp, and Kp interactions (see Sec. 2).

The preferred production of the resonances (item 2 in the list of general features) is due to the quark statistics of the additive quark model. It is a consequence of the assumption that quarks are combined into hadrons independently of the orientation of their spins. In this case, the number of $q\bar{q}$ pairs is proportional to the statistical weight $[2s(q\bar{q}) + 1]$ of these states and

$$\frac{n(q\bar{q},\ S=1)}{n(q\bar{q},\ S=0)} = 3:1. \tag{71}$$

This ratio holds for all particle-production regions and for all values of L $(q\bar{q})$. From this we obtain the preferred production of states with high spins in the framework of one $SU(6)$ multiplet. From (71) there follow numerous relationships between the yields of different hadrons, and these can be tested experimentally[18,33–35]:

$$\rho : \pi = 3 : 1;\ K^*(890) : K = 3 : 1;\ \Lambda^+ : p = 2 : 1, \tag{72}$$

etc. In Table III, the predictions of the additive quark model are compared with the data on the production of vector ($L = 0$) and tensor ($L = 1$) mesons in $K^{\pm}p$ interactions at $p = 32$ GeV/c. The agreement can be regarded as good, except for $\langle n(K^{\pm}(890))\rangle$, which is possibly due to their alignment or "contamination" by quasi-two-particle processes (see Sec. 2). Another example is given in Table X.[34,35] This gives the cross sections for production of strange resonances (K) in K^-p interactions ($p = 32$ GeV/c) and in pp collisions ($p = 405$ GeV/c) and their fractions in percentages. In the additive quark model it is expected that strange mesons are produced in 75% of the events with $S(q\bar{q}) = 1$ and in 25% of the events with $S(q\bar{q}) = 0$ [the relation (71)]. All particles with $S(q\bar{q}) = 1$ are resonances if we ignore the decays of nonstrange mesons into kaons. The vector mesons $K^*(890)$ belong to the lowest multiplet of mesons with $L = 0$, and the tensor mesons $K^*(1420)$ have $L = 1$. The tensor mesons are 5/12 of the particles of the $SU(6)$ multiplet with $L = 1$, i.e., $n(L = 1) = 12T/5$. Of them, 75% have $S(q\bar{q}) = 1$, i.e., $9T/5$. From this it is found that the number $V + 9T/5$ determines the number of states with $S(q\bar{q}) = 1$. As can be seen from Table X, to within the errors it is close to 75%.[9)] Thus, the main quark-statistics rule (71) of the additive quark model is well satisfied (see Sec. 2).

Thus, it was predicted[18] in the framework of the additive quark model in 1973 that there should be copious production of resonances in high-energy particle interactions, and this was discovered in 1976–1980 (item 2 in the list of general features).[5,7,11] The predictions of this model have now been verified in more detail, and to within 5% they agree with the experiments. In the additive quark model, the fraction of directly produced pions and kaons does not exceed 5%.[33] Of course, with the accumulation of data deviations from the model will undoubtedly be discovered. It is already possible to suggest numerous possible improvements of the model: allowance for polarization (alignment) of the resonances in the fragmentation region (see Sec. 2), the introduction of rapidity correlations between the quarks, allowance for the distributions of the constituent quarks in the hadrons, etc. (see Refs. 5, 7, and 34–36).

However, at the present time the model is adequate for the level of the available experimental data (see Secs. 3 and 2). In this connection, it can be assumed that the idea of

[9)] In this calculation, the contribution of the states with $L = 2$ was ignored. Estimates suggest that it is 5–10%.[34,35]

TABLE X. Production of kaons in K^-p interactions at $p = 32$ GeV/c and in pp collisions at 405 GeV/c (diffraction processes are eliminated).

Cross section	$K^-p \to K^-X$		$K^-p \to \bar{K}^0X$		$K^-p \to K^+X$		$K^-p \to K^0X$		$pp \to K^0_sX$	
	mb	%	mb	%	mb	%	mb	%	mb	%
Total	8.3±1.5	100	8±0.5	100	1.6±0.5	100	1.6±0.5	100	7.4±0.5	100
For vector mesons (V)	4±0.4	48	4.2±0.3	53	1.1±0.3	69	0.9±0.2	56	3.4±1.0	46
For tensor mesons (T)	0.9±0.2	11	0.8±0.2	10	0.08±0.1	5	0.08±0.01	5	1.7±0.8	23
For mesons with $L = 0$ [(4/3)V]	5.3±0.5	64	5.6±0.4	71	1.5±0.4	92	1.2±0.3	75	4.5±1.3	61
For mesons with $L = 1$ [(12/5)T]	2.2±0.5	25	1.9±0.5	24	0.19±0.02	12	0.19±0.02	12	4.1±1.9	55
For mesons with $L = 2$ (estimate)	—	11	—	5	—	—	—	13	—	—
For mesons with $S(q\bar{q}) = 1$ [V + (9/5)T]	5.6±0.4	68±5	5.6±0.3	71±4	1.24±0.3	72±19	1.04±0.2	6.5±13	6.5±1.8	87±24

almost free constituent quarks corresponds to reality.[10] This means that hadrons have two characteristic dimensions: r_q and R_h, where r_q is the radius of a constituent quark and R_h is the radius of the hadron. Estimates show that $r_q^2/R_h^2 \approx 0.1$ and $r_q \approx 2\times10^{-14}$ cm.[11,32–35] Thus, at $Q^2 \lesssim 1$ GeV^2 a constituent quark is not a single system but a "composite" system with the quantum numbers of the valence quark–parton. At $Q^2 \gtrsim 1$ GeV^2, its parton structure begins to be manifested, while at $Q^2 \gg 1$ GeV^2 we have point quark–partons. This agrees completely with the face that the characteristic transverse momenta of the partons in hadrons are fairly large (about 0.5–1 GeV), close to the reciprocal radius of a constituent quark (see Sec. 3).[5,32]

This picture is nontrivial because of the presence in QCD of a unique constant,which varies with the distance monotonically and cannot be large either at $r \approx r_q$ or at $r \sim R_h$. It is possible that the confinement of the "sea" of the constituent quark is ensured by the production of colorless gluonic formations—gluonium with $M(g) \approx 2$–3 GeV.[32,34,35]

We now consider the features of processes with large momentum transfers $Q^2 \gg 1$ GeV^2 (see Sec. 3). The entire difference from soft hadron collisions in the interpretation of these processes in the framework of the additive quark model is that initially point quarks are produced (see Fig. 17), these being transformed into constituent quarks as the process develops. They are then transformed into hadrons in accordance with the rules (65)–(68) of quark statistics. The proposed composition of the fragmenting quarks for different reactions is given in Table VI. The spectator quarks in lN interactions and in hard hadron collisions fragment in exactly the same way as in soft hadron collisions.

From the general picture we immediately deduce general features quark fragmentation in the considered processes and universality of hadron jets. Indeed, in the central region ($|x| \lesssim 0.15$) the hadron production mechanism depends neither on the species of the primary particles nor on the quantum numbers of the secondary hadrons, this being so for the same reasons as in soft hadron collisions. Of course, it is necessary to compare the characteristics of the hadron jets in different processes at the same jet energy (see Sec. 3). The multiplicity of the hadrons in this region increases with increasing energy in accordance with (65). This explains the growth of $\langle n_{ch} \rangle$ in the hadron jets (see Fig. 18). At sufficiently high energies, the growth of $\langle n_{ch} \rangle$ is expected to be the same for all types of interaction. All the other characteristics of the hadrons in this region should also be independent of the initial conditions (for example, $\psi(n/\langle n_{ch} \rangle)$, the composition of the particles, their distributions with respect to $p_\perp^2$, y etc.), as is indeed observed experimentally (see, Sec. 3). The universality and identity predicted by the additive quark model for the central hadron-production region in any type of interaction also ensures to a considerable degree the remarkable agreement between the characteristics of secondary hadrons produced in different processes that we discussed in Sec. 3 (item 3 of the general features).

In the fragmentation region of the knocked-out quarks ($|x| \gtrsim 0.15$) the characteristics of the long-lived hadrons in the jets are also similar, although the quark composition in different processes is different (see Table VI). In the additive quark model, the fragmentation mechanism for all quark species is assumed to be the same [see Eq. (67)].[34,35] There-

[10] An important argument for this structure of the hadrons is the successful application of the additive quark model to hadron–nucleus interactions.[11] On the other hand, some of the relations of the model can also be obtained in the framework of QCD.[76]

fore, the distributions of the hadrons with respect to x and $p_\perp^2$ are also expected to be the same (see Figs. 20–22) (item 3 of the general features). The ratios of the baryons to the mesons must also be the same, with $M{:}B = 2{:}1$ as in (69). A high proportion of baryons in jets was indeed found in e^+e^- annihilation, lN interactions, and hard hadron collisions (see Sec. 3).

The first data on the production of resonances in these processes show that their proportion is not less than in soft hadron collisions (see Table VII).

We shall compare the predictions of the additive quark model for the production of long-lived hadrons for the example of e^+e^- annihilation processes.[35] As a function of x, the cross section of these processes can be represented in the form

$$\frac{s}{\beta}\left(\frac{1}{2\sigma}\frac{d\sigma}{dx}(e^+e^-\to hX)\right) = \frac{1}{3}D_u(x)+\frac{1}{3}D_{\bar u}(x)+\frac{1}{12}D_d(x) + \frac{1}{12}D_{\bar d}(x)+\frac{1}{12}D_s(x)+\frac{1}{12}D_{\bar s}(x), \quad (73)$$

where $\sqrt{s}$ is the total energy of the e^+e^- annihilation, B is the c.m.s. velocity of the particle, $D_i(x)$ are the quark (and antiquark) fragmentation functions, and the factor $\frac{1}{2}$ arises because of the production of two jets. The experimental data were obtained at $\sqrt{s} = 4$–5 GeV, and therefore the production of heavier quarks (c, b) can be ignored. The calculations in the additive quark model were made with allowance for only the lowest $SU(6)$ multiplets of hadrons with $L = 0$. The fragmentation functions $D_i(x)$ were assumed to be the same for all types of quarks and antiquarks[35]:

$$D_i(x) = \frac{1}{3}F_B(x)+\frac{2}{3}\Phi_M(x)+N(s)\,(6\varphi_M(x)+f_B(x)), \quad (74)$$

where $F_B(x)$ and $\Phi_M(x)$ are the fragmentation functions of the baryons (and antibaryons) and mesons in the fragmentation region, and $\varphi_M(x)$ and $f_B(x)$ are the functions in the central region. The integrals over these functions in the complete range of x are normalized to unity. The coefficients in (74) correspond to the rules (65) and (67) of quark statistics in the additive quark model. As a rule, the choice of the quark (and antiquark) fragmentation functions is based either on existing data on their distributions with respect to x in nucleons (see Fig. 14),[2] or on experimental data on quark fragmentation.[2,34–36] At the present level of experiments their actual form is rather arbitrary, except for the regions $x\to 0$ and $x\to 1$. In the region $x\to 0$, hadron production from sea quarks is predominant, and therefore $\varphi_M(x)\sim f_B(x)\sim 1/x$.[2,35] In the region $x\to 1$, the hadron distributions are related to the behavior of the hadron form factors, and $\Phi_M\sim(1-x)$ and $F_B(x)\sim(1-x)^3$.[2,35]

To describe e^+e^- annihilation, the following function was used:

$$\Phi_M(x) = \frac{1-x}{\sqrt{x}}(A_M + B_M x + C_M x^2), \quad (75)$$

where $\sqrt{x}$ takes into account the suppression of the probability of finding in a meson in the limit $x\to 0$ a valence quark compared with a sea quark; the coefficients A, B, C of the polynomial were determined from experiment. A difference between $F_B(x)$ and $\Phi_M(x)$ appears only in the region $x \gtrsim 0.9$ because of the different behavior of the baryon form factors:

$$F_B(x) = \frac{\Phi_M(x)}{1+\alpha/(1-x)^2} \quad (76)$$

and $F_B(x)\sim(1-x)^3$ as $x\to 1$ ($\alpha = 0.1$). In the central region, $\varphi_M(x)\sim f_B(x)\sim 1/x$ as $x\to 0$. For this choice of the fragmentation functions, the distributions (73) and (74) with respect to x of the directly produced particles were found, and then their decay into long-lived mesons and baryons was taken into account. The results of calculations in accordance with the additive quark model satisfactorily describe the experimental data (see Fig. 22). This means that the quark-statistics rules (74) are also satisfied in the first approximation for e^+e^- annihilation.

The similarity of the characteristics of hadrons in all types of particle interaction can also be explained qualitatively in the additive quark model. In this case, the separation of the leading particles ($|x|\approx 0.4$) in soft collisions means that fragmentations hadrons are eliminated and there remain only the hadrons produced in the central region (see Fig. 24). As we have already noted, the behavior of the hadrons in this region depend neither on the species of the primary particles nor on the type of their interaction.

Recently, fragmentation functions have also been introduced in the framework of the model for soft hadron collisions, which makes it possible not only to describe the general features of these processes but also to make a quantitative comparison of the momentum spectra of the secondary particles with the predictions of the model.[34,35]

Thus, in the framework of the additive quark model one can describe many phenomena ranging from the static properties of the hadrons and the relationships between their total interaction cross sections to the characteristics of hadron jets in processes with large momentum transfers. The introduction of the fragmentation functions (75) and (76) essentially completes the construction of a complete phenomenological model describing the hadrons and their production in interactions of high-energy particles. For comparison, we give the main postulates of the Field–Feynman model, which is widely used to describe hard hadron collisions.[2] Conceptually, it is quite different from the additive quark model. In it, one considers the fragmentation of current quarks into hadrons without the stage in which the constituent quarks are produced (as in the additive quark model). However, the fragmentation functions in both models are taken on the basis of the same experimental data, and therefore the final results must agree. In the Field–Feynman model, the quark–meson fragmentation function ($D_q^M(x)$) has the form[11)]

$$D_q^M(x) = \frac{\varphi_1(a)}{x}+\varphi_2(a)\,x+\varphi_3(a)\,x^{2(1-a)}, \quad (77)$$

where the functions $\varphi_i(a)$ and the parameter $a = 0.77$ are determined from the experimental data on e^+e^- annihilation and deep inelastic lN interactions. The distribution of the directly produced mesons with respect to the transverse momenta relative to the jet axis is taken in the Gaussian form

[11)] Very often, the following form of the scaling functions is used:

$$D_q^M(z) = 1-a+3a(1-z)^2,$$

where $z = \frac{E+p)h}{(E+p)q}$

$$\frac{dN(M)}{dp_\perp^2} = A\exp(-p_\perp^2/2\sigma^2) \quad (78)$$

and $\langle p_\perp \rangle = (\sqrt{\pi}/2)\sigma$ the value $\sigma \approx 0.35$–0.04 GeV/c is taken to make the primary mesons have $\langle p_\perp(R)\rangle = 0.45$–$0.50$ GeV/c and $\langle p_\perp(\pi^+)\rangle = 0.32$–$0.35$ GeV/c (see Secs. 2 and 3). In addition, one also specifies in the model the branching ratio of the production of vector (V) and pseudoscalar (P) mesons (V:P = 1:1) and the degree of breaking of $SU(3)$ symmetry in the production of $s\bar{s}$ quark pairs $(u\bar{u}):(s\bar{s}) = 2:1$).[12] It is assumed that after each meson emission the kinematic characteristics of the subsequent fragmentation process (77) and (78) remain unchanged. It can be seen that the basic assumptions of this model are approximately the same as in the additive quark model, except for the quark statistics. The V:P ratio in this model is taken from experimental data, which are obtained with large errors and hardly correspond to the true ratio of the initial mesons (see Tables V and VII). In the model, one cannot describe the production of baryons, though there are attempts to modify it in this direction.[77]

On the basis of this model, the Monte Carlo method was used to obtain typical hadron jets and study their characteristics, i.e., the inclusive distributions of the mesons, the correlations between them, the charge distributions of the hadrons as functions of x, etc.[2] The results of these calculations are widely used to describe the characteristics of hadron jets in hard and soft hadron collisions and to determine more accurately the chosen parameters of the model.[48,72]

A comparison of the predictions of the additive quark model and the Field–Feynman model for hard hadron collisions has not yet been made. In a first approximation, their basic assumptions are similar, and the experimental data are obtained with large errors. This applies especially to the distributions with respect to x and $p_\perp^2$ of the directly produced particles (the resonances).

As data are accumulated, the parameters of these models will be determined more accurately—they must also be obtained in the framework of QCD.

CONCLUSIONS

Study of the production of resonances and hadron jets in high-energy particle interactions has significantly changed our ideas about the structure of hadrons and their interactions.

These investigations have revealed copious production of resonances and a universality of their production mechanism (see Sec. 2). It has been found that the characteristic transverse momentum of hadron production is $\langle p_\perp(R)\rangle \approx 0.5$ GeV/c, and not $\langle p_\perp(\pi)\rangle \approx 0.34$ GeV/c, as was assumed earlier. The secondary long-lived hadrons are largely decay products of the resonances, and therefore reflect the interaction dynamics weakly. It is evident that the hadrons have two characteristic dimensions: $R_h \sim 1/2m_\pi$ and $r_q \sim 1/m_N$. The latter is associated with the existence of new objects—constituent quarks within hadrons, which are as yet absent in QCD. It is possible that these objects are associated with colorless formations of gluons with $M(g) = 2$–3 GeV, intense searches for which are now being made.

In a first approximation, the characteristics of hadrons in jets also depend weakly on the type of interaction and have a simple scaling behavior, despite the different composition of the fragmenting quarks (see Sec. 3).

Of course, as experimental data are accumulated we expect a differentiation of the hadron jets in accordance with the species of the fragmenting quarks (see Secs. 3 and 4). In this connection, we need new experiments both in the region of energies $\sqrt{s} \lesssim 60$ GeV and at collider energies ($\sqrt{s} = 0.5$–2 TeV).

The quark–parton models (see Sec. 4) satisfactorily describe the available data with the introduction of phenomenological parameters, which must be obtained in the complete theory of the strong interactions.

I should like to thank R. A. Kvatadze, R. Lednicky, and Yu. M. Shabel'skii for helpful discussions.

[12]In the additive quark model, V:P = 3:1 (72) and $(u\bar{u}):(s\bar{s}) = 3:1$.

[1]L. B.Okun', Leptony i kvarki, Nauka, Moscow (1981); English translation: Leptons and Quarks, North-Holland, Amsterdam (1982); Usp. Fiz. Nauk **134**, 3 (1981) [Sov. Phys. Usp. **24**, 341 (1981)].

[2]R. P. Feynman, Photon–Hadron Interactions, Addison-Wesley, Reading, Mass. (1972) (Russian translation published by Mir, Moscow (1975)); R. P. Feynman *et al.*, Phys. Rev. D **18**, 3320 (1978); R. D. Field and R. P. Feynman, Nucl. Phys. **B136**, 1 (1978).

[3]V. S. Murzin and L. I. Sarycheva, Kosmicheskie luchi i ikh vzaimodeĭstvie (Cosmic Rays and Their Interactions), Atomizdat, Moscow (1968); S. I. Nikol'skiĭ, Usp. Fiz. Nauk **135**, 545 (1981) [Sov. Phys. Usp. **24**, 925 (1981)].

[4]E. L. Feĭnberg, Usp. Fiz. Nauk **132**, 255 (1980); **139**, 3 (1983) [Sov. Phys. Usp. **23**, 629 (1980); **26**, (1983)]; I. M. Dremin and E. L. Feĭnberg, Fiz. Elem. Chastits At. Yadra **10**, 996 (1979) [Sov. J. Part. Nucl. **10**, 394 (1979)].

[5]V. G. Grishin, Inklyuzivnye protsessy v adronnykh vzaimodeĭstviyakh pri vysokikh énergiyakh (Inclusive Processes in High Energy Hadron Interactions), Énergoizdat, Moscow (1982); V. G. Grishin, Usp. Fiz. Nauk **127**, 51 (1979) [Sov. Phys. Usp. **22**, 1 (1979)]; Fiz. Elem. Chastits At. Yadra **7**, 595 (1976) [Sov. J. Part. Nucl. **7**, 233 (1976)].

[6]V. S. Murzin and L. I. Sarycheva, Mnozhestvennye protsessy pri vysokikh énergiyakh (Multiparticle Production Processs at High Energies), Atomizdat, Moscow (1974).

[7]A. K. Likhoded and P. V. Shlyapnikov, Usp. Fiz. Nauk **124**, 3 (1978) [Sov. Phys. Usp. **21**, 1 (1978)]; P. V. Chliapnikov, in: Proc. of the 11th Intern. Symposium on Multiparticle Dynamics, Bruges, Belgium (1980), p. 232.

[8]I. V. Andreev and I. M. Dremin, Usp. Fiz. Nauk **122**, 37 (1977) [Sov. Phys. Usp. **20**, 381 (1977)].

[9]Yu. P. Nikitin and I. L. Rozental', Teoriya mnozhestvennykh protsessov (Theory of Multiparticle Processes), Atomizdat, Moscow (1976).

[10]L. Van Hove, Preprint CERN TH-3133 (1981).

[11]Yu. M. Shabel'skiĭ, Fiz. Elem. Chastits At. Yadra **12**, 1070 (1981) [Sov. J. Part. Nucl. **12**, 430 (1981)]: N. N. Nikolaev, Usp. Fiz. Nauk **134**, 369 (1981) [Sov. Phys. Usp. **24**, 531 (1981)].

[12]G. Ranft and J. Ranft, Fiz. Elem. Chastits At. Yadra **10**, 90 (1979) [Sov. J. Part. Nucl. **10**, 35 (1979)].

[13]P. V. Ermolov and A. I. Mukhin, Usp. Fiz. Nauk **124**, 385 (1978) [Sov. Phys. Usp. **21**, 185 (1978)]; V. M. Shekhter, Usp. Fiz. Nauk **119**, 593 (1976) [Sov.Phys. Usp. **19**, 645 (1976)]; T. H. Burnett *et al.*, Phys. Lett. **B77**, 443 (1978).

[14]E. De Wolf and F. Verbeure, in: Proc. of the 11th Intern. Symposium on Multiparticle Dynamics, Bruges, Belgium (1980), p. 125.

[15]J. Kirkby, in: SLAC-Pub-2419, Ocotber (1979) (Invited Talk at the Ninth Intern. Symposium on Lepton and Photon Interactions at High Energies, Batavia, Ill. (August 23–29, 1979) [Russian translation published in Usp. Fiz. Nauk **133**, 309 (1981)].

[16]G. Wolf, DESY 80/85, Hamburg (1980); K. H. Mess and B. H. Wiik, DESY 82-011, Hamburg (1981).

[17]C. Brieman *et al.*, Rev. Mod. Phys. **52**, 3 (1980).

[18]V. V. Anisovich and V. M. Shekhter, Nucl. Phys. **55**, 455 (1973).

[19]V. G. Grishin, in: Tr. XVIII Mezhdunarodnoĭ konferentsii po fizike vysokikh énergiĭ (Proc. of the 18th Intern. Conf. on High Energy Phys

ics), Vol. 1, Tbilisi (1976); Preprints D1,2-10400, A2-6 [in Russian], JINR, Dubna (1977); N. S. Angelov *et al.*, Preprint 1-9536 [in Russian], JINR, Dubna (1976); Yad. Fiz. **25**, 117 (1977); **33**, 1539 (1981) [Sov. J. Nucl. Phys. **25**, 63 (1977): **33**, 828 (1981)].
[20]M. Deutschmann *et al.*, Nucl. Phys. **B103**, 426 (1976).
[21]H. Grassler *et al.*, Nucl. Phys. **B132**, 1 (1978).
[22]G. Jancso *et al.*, Nucl. Phys. **B124**, 1 (1977).
[23]M. G. Albrow *et al.*, Nucl. Phys. **B155**, 39 (1979).
[24]P. D. Higgins *et al.*, Phys. Rev. D **19**, 65 (1979).
[25]Yu. M. Antipov *et al.*, Preprint 79-178 [in Russian], Institute of High Energy Physics, Serpukhov (1979).
[26]J. Bartke *et al.*, Nucl. Phys. **B137**, 189 (1978); M. Walter *et al.*, Z. Phys. **C3**, 89 (1979).
[27]R. Göttgens *et al.*, Z. Phys. **C9**, 21 (1981); I. V. Azhinenko *et al.*, Preprint 80-84 [in Russian], Institute of High Energy Physics, Serpukhov (1980); I. V. Ajinenko *et al.*, Nucl. Phys. **B165**, 1 (1980); R. T. Ross, CERN/EP 81-89, Geneva (1981); P. V. Shlyapnikov *et al.*, Preprint 81–71 [in Russian], Institute of High Energy Physics, Serpukhov (1981).
[28]P. Sixel *et al.*, Nucl. Phys. **B159**, 125 (1979).
[29]D. Drijard *et al.*, Z. Phys. **C9**, 293 (1981); C. Kourkoumelis *et al.*, Phys. Lett. **B91**, 481 (1980).
[30]H. Kichimi *et al.*, Phys. Rev. D **20**, 37 (1979).
[31]R. Webb *et al.*, Phys. Lett. **B55**, 331 (1975).
[32]V. M. Shekhter, Yad. Fiz. **33**, 817 (1981) [Sov. J. Nucl. Phys. **33**, 426 (1981)].
[33]V. M. Shekhter and L. M. Shcheglova, Yad. Fiz. **27**, 1070 (1978) [Sov. J. Nucl. Phys. **27**, 567 (1978)].
[34]V. V. Anisovich, M. N. Kobrinskiĭ, and J. Nyiri, Yad. Fiz. **34**, 195, 1576 (1981) [Sov. J. Nucl. Phys. **34**, 111, 875 (1981)].
[35]V. V. Anisovich, Yu. Nyiri, *et al.*, KFKI-56, Budapest (1981); KFKI-36, Budapest (1982).
[36]R. V. Hwa, Preprint OITS-165, University of Oregon, Oregon (1981).
[37]I. V. Azhinenko *et al.*, Preprint 81-139 [in Russian], Institute of High Energy Physics, Serpukhov (1981).
[38]J. F. Gunion, Phys. Lett. **B88**, 150 (1979).
[39]V. V. Knyazev *et al.*, Preprint 80-122 [in Russian], Institute of High Energy Physics, Serpukhov (1980).
[40]M. Basile *et al.*, CERN-EP/81-86, Geneva (1981).
[41]V. A. Matveev, R. Muradyan, and A. N. Tavkhelidze, Nucl. Phys. **7**, 719 (1973).
[42]K. J. Biebl *et al.*, Fortschr. Phys. **28**, 123 (1980).
[43]S. V. Dzhmukhadze *et al.*, Yad. Fiz. **33**, 160 (1981) [Sov. J. Nucl. Phys. **33**, 81 (1981)]; A. N. Aleev *et al.*, Preprint R1-81-165 [in Russian], JINR, Dubna (1981); Preprint R1-82-360 [in Russian], JINR, Dubna (1981).
[44]M. L. Faccini-Turluer *et al.*, Z. Phys. **C1**, 19 (1979); M. Barth *et al.*, Z. Phys. **C10**, 205 (1981).
[45]C. Wilkinson *et al.*, Phys. Rev. Lett. **46**, 803 (1981); S. Erhan *et al.*, Phys. Lett. **B82**, 301 (1979).
[46]V. Blobel *et al.*, Phys. Lett. **B48**, 73 (1973).
[47]B. V. Batyunya *et al.*, Czech. J. Phys. **B31**, 1353 (1981); D. I. Ermilova *et al.*, Preprint E1-11190 [in English], JINR, Dubna (1978).
[48]R. Sosnowski, in: Proc. of the 19th Intern. Conf. on High Energy Physics, Tokyo (1978), p. 693; P. Darriulat, Ann. Rev. Nucl. Sci. **30**, 159 (1980).
[49]C. Kourkoumelis *et al.*, Phys. Lett. **B84**, 271 (1979).
[50]M. Diakonou *et al.*, Phys. Lett. **B89**, 432 (1980); G. J. Donaldson *et al.*, Phys. Rev. D **21**, 828 (1980).
[51]A. Chilingarov *et al.*, Nucl. Phys. **B151**, 29 (1979).
[52]L. Van Hove, Sov. Phys. Usp. **21**, 252 (1978) (not published elsewhere).
[53]H. J. Lubatti, CERN-EP/81-64, Geneva (1981).
[54]G. Wolf, DESY 81-086, Hamburg (1981); 82-077, Hamburg (1982).
[55]M. Derrick *et al.*, Phys. Rev. D **24**, 1071 (1981); Phys. Lett. **B91**, 307 (1980).
[56]P. Allen *et al.*, Nucl. Phys. **B194**, 373 (1982).
[57]C. Papa *et al.*, Phys. Rev. Lett. **40**, 90 (1978); J. J. Aubert *et al.*, Phys. Lett. **B100**, 433 (1981).
[58]J. P. Berge *et al.*, Phys. Rev. D **22**, 1043 (1980).
[59]H. Grassler *et al.*, Nucl. Phys. **B194**, 1 (1982).
[60]M. Derrick *et al.*, Phys. Rev. D **17**, 1 (1978); S. J. Barish *et al.*, Phys. Rev. Lett. **45**, 783 (1980).
[61]V. V. Ammosov *et al.*, Nucl. Phys. **B177**, 365 (1981); **B162**, 205 (1980).
[62]R. G. Hicks *et al.*, Phys. Rev. Lett. **45**, 765 (1980).
[63]I. Cohen *et al.*, Phys. Rev. Lett. **40**, 1614 (1978).
[64]K. G. Chetyrkin *et al.*, Phys. Lett. **B85**, 277 (1979).
[65]J. Ellis *et al.*, Nucl. Phys. **B111**, 253 (1976).
[66]R. Brandelik *et al.*, Nucl. Phys. **B148**, 189 (1979); Phys. Lett. **B86**, 243 (1979); W. Bartel *et al.*, Phys. Lett. **B91**, 142 (1980).
[67]R. Brandelik *et al.*, Phys. Lett. **B97**, 453 (1980); H. J. Behrend *et al.*, DESY 81/80, Hamburg (1981).
[68]R. Brandelik *et al.*, Phys. Lett. **B89**, 418 (1980); M. Basile *et al*, Phys. Lett. **B95**, 311 (1980); CERN-EP/81-76, Geneva (1981).
[69]W. Furmanski *et al.*, Nucl. Phys. **B155**, 253 (1979).
[70]K. Alpgard *et al.*, Phys. Lett. **B107**, 310 (1981).
[71]R. Brandelik *et al.*, Phys. Lett. **B92**, 199 (1980); **B105**, 75 (1981); DESY-81/69, Hamburg (1981).
[72]M. Barth *et al.*, Nucl. Phys. **B192**, 289 (1981); V. G. Grishin, L. A. Didenko, and T. Kanarek, Preprint R1-81-542 [in Russian], JINR, Dubna (1981).
[73]M. Basile *et al.*, Phys. Lett. **B95**, 311 (1981); **B92**, 367 (1980); CERN/EP 80-111, Geneva (1980); CERN/EP 81-102, Geneva (1981); CERN/EP 81-43 (1981); Nuovo Cimento **A67**, 53 (1982).
[74]A. Breakstone *et al.*, CERN/EP 81-68, Geneva (1981).
[75]R. Horgan and M. Jacob, "Physics at collider energy," (originally a CERN publication, 1981), Usp. Fiz. Nauk **136**, 219 (1982) [no English version published in Sov. Phys. Usp.].
[76]E. M. Levin and M. G. Ryskin, Yad. Fiz. **34**, 1114 (1981) [Sov. J. Nucl. Phys. **34**, 619 (1981)].
[77]T. Mayer, DESY 81-46, Hamburg (1981).

Translated by Julian B. Barbour